Article

Not peer-reviewed version

Search for Potential Neuroprotectors for Correction of Cognitive and Behavioral Disorders After Ketamine Anesthesia Among 2′-R-6’H-Spiro(cycloalkyl-, heterocyclyl)[1,2, 4]triazolo[1,5-C]-Quinazolines: Fragment-Oriented Design, Molecular Docking, ADMET, Synthesis and *In Vivo* Study

Kostiantyn Shabelnyk *, Lyudmyla Antypenko, Natalia Bohdan, Victor Ryzhenko, Igor Belenichev, Oleksandr Kamyshnyi *, Valentyn Oksenych *, Serhii Kovalenko

Posted Date: 4 April 2025

doi: 10.20944/preprints202504.0388.v1

Keywords: 2'-R-6'H-spiro(cycloalkyl-, heterocyclyl)-[1,2,4]triazolo[1,5-c]quinazolines; neuroprotective activity; molecular docking; synthesis; ADMET; SAR

 doi:10.20944/preprints202504.0388.v1

Article

Search for Potential Neuroprotectors for Correction of Cognitive and Behavioral Disorders After Ketamine Anesthesia Among 2'-R-6'*H*-Spiro(cycloalkyl-, heterocyclyl)[1,2,4]triazolo[1,5-*c*]-quinazolines: Fragment-Oriented Design, Molecular Docking, ADMET, Synthesis and *In Vivo* Study

Kostiantyn Shabelnyk [1,*], Lyudmyla Antypenko [2], Natalia Bohdan [3], Victor Ryzhenko [1], Igor Belenichev [1], Oleksandr Kamyshnyi [4,*], Valentyn Oksenych [5,*] and Serhii Kovalenko [6]

[1] Zaporizhzhia State Medical and Pharmaceutical University, 26 Maria Primachenko Blvd., 69035, Zaporizhzhia, Ukraine
[2] Independent Researcher, Lamana Str. 11, 69063, Zaporizhzhia, Ukraine
[3] Institute of Organic Chemistry of the National Academy of Sciences of Ukraine, 5 Akademika Kukharya Str., 02094, Kyiv, Ukraine
[4] Department of Microbiology, Virology and Immunology, I. Horbachevsky Ternopil State Medical University, 46001 Ternopil, Ukraine
[5] Department of Clinical Science, University of Bergen, 5020 Bergen, Norway
[6] Institute of Chemistry and Geology, Oles Honchar Dnipro National University, 72, Nauki Ave., 49010, Dnipro Ukraine
* Correspondence: kshabelnik@gmail.com (K.S.); kamyshnyi_om@tdmu.edu.ua (O.K.); valentyn.oksenych@uib.no (V.O.)

Abstract: Background/Objectives: Ketamine anesthesia frequently causes postoperative cognitive dysfunction and behavioral disorders, with limited effective therapeutic options. This study explores novel neuroprotective compounds targeting multiple pathways in neurological disorders following ketamine anesthesia through the design, synthesis, and evaluation of 2'-R-6'*H*-spiro(cycloalkyl-, heterocyclyl)[1,2,4]triazolo[1,5-*c*]-quinazolines. **Methods:** Using fragment-oriented design, we synthesized 40 spiro-triazoloquinazolines *via* [5+1]-cyclocondensation. Molecular docking assessed binding affinities to glutamate receptor GluA3, while ADMET analyses evaluated pharmacokinetic properties. Selected compounds were tested in a ketamine-induced cognitive impairment rat model with behavioral assessment via open field test. Neurobiochemical analyses measured inflammatory markers, apoptotic regulators, and gene expression in hippocampal tissue. **Results:** Molecular docking showed superior binding affinities to GluA3 compared to reference nootropics, while ADMET analyses confirmed favorable drug-likeness profiles. *In vivo* evaluation demonstrated compounds **25**, **26**, and **32** effectively normalized ketamine-disrupted behavioral parameters, reducing anxiety and improving cognitive function more effectively than piracetam and fabomotizole. Neurobiochemical analyses revealed compound-specific mechanisms: compound **31** showed potent anti-inflammatory effects (72% reduction in IL-1β, 80% reduction in caspase-1), while compound **26** enhanced cell survival pathways (96% increase in Bcl-2) and hypoxic adaptation (3.5-fold increase in HIF-1 mRNA). Structure-activity relationship analyses established that spiro-junction type and 2'-position substituent critically determine pharmacological profiles. **Conclusions:** These novel spiro-triazoloquinazolines demonstrate promising neuroprotective properties for treating cognitive and behavioral disorders associated with ketamine anesthesia through multiple mechanisms including anti-inflammatory, anti-apoptotic, and adaptive pathway modulation. Their superior efficacy compared to current treatments positions them as candidates for further

 doi:10.20944/preprints202504.0388.v1

development in post-anesthetic cognitive dysfunction and potentially in post-viral and trauma-related neurological conditions.

Keywords: 2'-R-6'*H*-spiro(cycloalkyl-, heterocyclyl)-[1,2,4]triazolo[1,5-*c*]quinazolines; neuroprotective activity; molecular docking; synthesis; ADMET; SAR

1. Introduction

Ketamine is a dissociative anesthetic widely used in medicine for the induction and maintenance of anesthesia. Ketamine anesthesia is applied in military field surgery because it enables simultaneous anesthesia for multiple patients and can save the lives of a significant number of casualties [1,2]. However, in military medicine, ketamine is not recommended for high-ranking officers due to concerns, that it may impair their professionalism and, consequently, lead to inadequate command decisions [3,4].

Currently, it is impossible to abandon ketamine due to its numerous positive properties. The drug remains the safest general anesthetic, unlike all other anesthesiologic agents, as it uniquely stimulates and supports the cardiovascular and respiratory systems [5]. Furthermore, many psychiatric side effects of ketamine can now be successfully managed, primarily through the use of neuroleptics (butyrophenone derivatives, benzodiazepines, and others), that correct unwanted changes [6,7].

However, the main problem with ketamine use is not related to intraoperative undesirable hemodynamic changes, but rather to long-term disturbances in the psycho-emotional sphere (sometimes lasting up to six months after ketamine anesthesia) [8]. Typically, such patients are not monitored by physicians after surgery, and subsequent deterioration of their cognitive functions and emotional state is rarely associated with ketamine's side effects.

Ketamine anesthesia can cause central nervous system (CNS) damage in the postoperative period, with postoperative cognitive dysfunction (POCD) being particularly significant. POCD can develop in patients of various age groups with no history of psychoneurological conditions. According to various authors [9–12], the frequency of POCD averages 36.8% of patients overall, ranges from 3% to 47% after cardiac surgery (with 42% of patients still affected 3-5 years after surgery), and from 7% to 26% after non-cardiac surgery (with 9.9% of patients affected for 3 months or more, and 1% of patients for over 2 years). Early POCD can lead to deterioration in patients' quality of life, specifically reducing their professionalism and level of socialization [13,14].

Among medications used to restore the psycho-emotional sphere in the postoperative period, piracetam is administered toward the end of surgery. However, there are extremely few other studies exploring pharmacological correction of POCD after ketamine. A neuroprotection concept has been proposed for POCD, aimed at timely restoration of neurochemical processes, cerebral hemodynamics, and elimination of cognitive-mnestic disorders [15]. The complexity of developing staged neuroprotection after POCD lies precisely in the lack of exact knowledge about the subtle mechanisms of ketamine's neurotoxic action.

Our earlier research and data from other investigators have established that ketamine causes activation of ROS production through increased expression of i-NOS and n-NOS, neuroinflammation, dysfunction of neuronal mitochondria, initiation of neuroapoptosis, and consequently, deterioration of spatial and working memory, increased anxiety, and more episodes of depressive behavior [16,17].

Currently, several nootropics have been proposed for POCD correction, including phenibut, ipacridine, cytoflavin, noopept, cerebrocurin, and thiocetam [18,19]. However, modern nootropic agents and neurometabolic neuroprotectors do not fully resolve the POCD problem. Racetams (piracetam, phenotropil, pramiracetam) enhance anxiety and positively modulate anaerobic glycolysis in neurons, which exacerbates lactate acidosis. Cerebrocurin provides rapid metabolic effects, activates energy metabolism, reduces neuroapoptosis and mitochondrial dysfunction, but

 doi:10.20944/preprints202504.0388.v1

does not affect amino-specific CNS systems such as GABA and serotonin, which play critical roles in the formation of anxiety, sadness, worry, anger, and emotional numbness [20–22].

All this necessitates the development and creation of entirely new structures that would have affinity for GABA and 5HT2A receptors, influence genes associated with the expression of specific amino-specific system intermediates and the function of the hypothalamic-pituitary-adrenal axis, as well as impact structural and functional abnormalities in the hippocampus, prefrontal cortex, amygdala, and other brain regions [23–25]. Currently, developing more effective medications with improved safety profiles to enhance cognitive function and treat anxiety disorders is an important task in medicinal chemistry.

The stress response system involves several key receptor interactions in war-related PTSD. CRF1R is directly involved in stress response and anxiety. GABA(A) receptors are crucial for anxiety management and sleep disturbances. Serotonin receptors play key roles in mood regulation and traumatic memory processing. The complex symptomatology of PTSD involves multiple receptor systems, that are interconnected in addressing various symptoms: sleep disturbances (5-HT7, GABA(A)), hyperarousal (CRF1R, GABA(A)), depression (D2, 5-HT1A), anxiety (GABA(A), 5-HT1A), and cognitive issues (GluA3, M2).

In terms of treatment potential, a multi-target approach might be more effective for complex conditions like PTSD. Understanding receptor interactions could lead to more effective therapeutic strategies, with the potential for developing medications that address multiple symptoms simultaneously.

Based on the aforementioned considerations, our rational drug design strategy was directed toward combining the key structural features of various chemical classes of clinically confirmed pharmacophores (Figure 1, Table 1) and optimizing their molecules with saturated structural elements to increase lipophilicity and minimize toxicity.

Analysis of these reference compounds reveals essential pharmacophoric elements required for optimal nootropic and anxiolytic activity:

Core Structure Requirements

- Essential azoheterocyclic core
- *N*-methyl group for optimized GABA-A receptor binding
- Strategically positioned cycloalkyl/heterocyclyl rings for receptor pocket compatibility

Linking Elements

- Azapirone structure with piperazine linker
- Specific alkylated terminal rings (pyrimidine, piperidine, pyridine, etc.)
- Optimal four-carbon spacing between cyclic systems

Stability and Binding Elements

- Cycloalkyl/alkyl groups for metabolic stability
- Multiple hydrogen bond donors/acceptors
- Flexible alkyl chains for conformational adaptation

Pharmacokinetic Considerations

- Balanced lipophilicity for blood-brain barrier penetration

Table 1. Chemical classes of clinically confirmed pharmacophores selected for drug design according to the protein data bank targets.

Compounds	Structural features	Mechanism of activity*	Pharmacological effect
Diazepam	benzodiazepine	GABA-A receptor positive allosteric modulator (α1/β3/γ2L)	sedative and muscle relaxant (anxiolytic) [26]
AFDX-384	benzodiazepine	muscarinic acetylcholine receptor antagonist (M_2 and M_4 subtypes)	treatment of dementia and schizophrenia [27]

 doi:10.20944/preprints202504.0388.v1

Piracetam	pyrrolidine	AMPA receptor positive modulator and influences membrane fluidity, affecting ion transport and mitochondrial function	ootropic, used in cognitive impairment and myoclonus [28]
Pramiracetam	pyrrolidine	glutamate receptor 3 (GluA3)	nootropic stimulant [29]
SB-269970	pyrrolidine	selective 5-HT$_7$ receptor antagonist	treatment of anxiety and depression and nootropic effects [30]
Mavoglurant	indole	antagonist of the metabotropic glutamate receptor 5 (mGluR5)	obsessive-compulsive disorder [31]
Fabomotizole	benzimidazole	Selective MT3 (sigma-1) receptor ligand with anxiolytic properties	anxiolytic and neuroprotective agent [32]
CP-154,526	pyrrolo[3,2-*e*]-pyrimidine	corticotropin-releasing factor receptor 1 (CRF1R)	treatment of alcoholism [33]
JWH-133	tetrahydrobenzo[*c*]–chromene	cannabinoid (CB$_2$) receptor agonist, G protein coupled receptor	anxiolytic [34]
Buspirone	azaspiro[4.5]decane	serotonin 5-HT$_{1A}$ receptor partial agonist	anxiolytic (treat anxiety disorders) [35]
Risperidone	1,2-benzoxazol; pyrido[1,2-*a*]–pyrimidine	5-HT (5-HT$_{2C}$, 5-HT$_{2A}$) receptors antagonist, D2 dopamine receptor	antipsychotic, anxiolytic [36]

*GABA-A: gamma-aminobutyric acid type A receptor; AMPA: α-amino-3-hydroxy-5-methyl-4-isoxazole propionic acid receptor; 5-HT: 5-hydroxytryptamine (serotonin) receptor; mGluR5: metabotropic glutamate receptor 5; CRF1R: corticotropin-releasing factor receptor 1; CB$_2$: cannabinoid receptor type 2. Target selection was guided by relevance to cognitive enhancement, anxiety modulation, and neuroprotection. Structural features were analyzed to identify key pharmacophoric elements essential for receptor binding and biological activity.

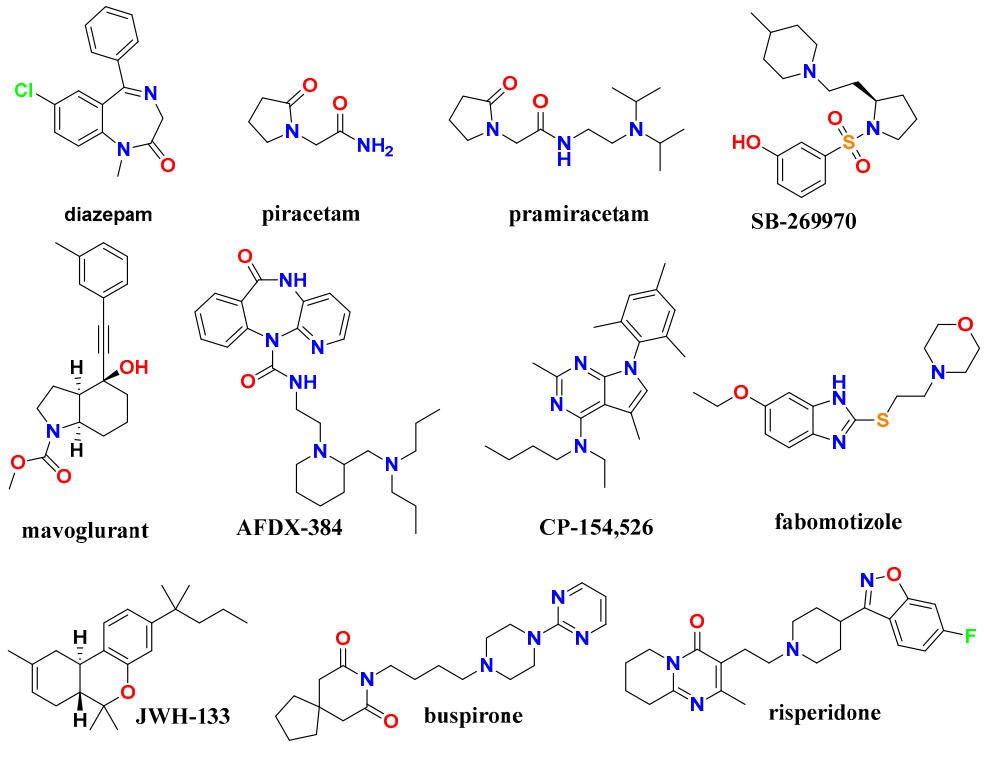

Figure 1. Nootropic and anxiolytic reference compounds chosen for rational drug design.

 doi:10.20944/preprints202504.0388.v1

The foundation of our rational design for promising bioactive substances is based on the modern experience of merging molecular fragments through spiro-conjunction. Moreover, azaheterocycles fused with spirocyclic fragments represent an exceptional tool in drug development, allowing for the adjustment of conformational and physicochemical properties of the investigated molecule [37–39].

The main advantage characteristic of this class of compounds is their inherent three-dimensional nature, which is beneficial for ligand interactions with the three-dimensional binding site of a biotarget. Another advantage is their solubility, which is associated with the high content of sp^3-hybridized Carbon atoms. Importantly, this advantage liberates "lead compounds" from many pharmaco-technological and pharmacokinetic obligations that arise when implementing typical aromatic or heterocyclic structures. Furthermore, spiroheterocycles exhibit a broad spectrum of biological activities, including anti-inflammatory, anticonvulsant, antiproliferative, antimalarial, antimicrobial, and other types of activity [37–42].

Therefore, the fusion of two molecular fragments was decided to be conducted via a 5+1-heterocyclization reaction involving triazoloanilines and cycloalkanones (Figure 2). We believe that the high content of sp^3-hybridized Carbon atoms will not only improve drug-likeness criteria but also provide additional binding to molecular targets and lead to improved toxicological parameters.

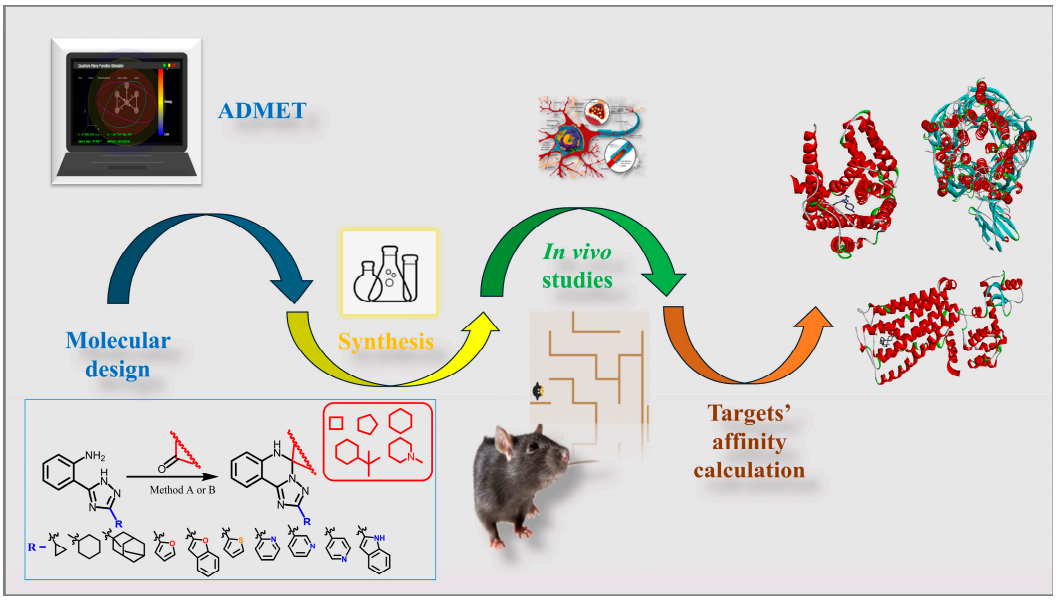

Figure 2. Design and research methodology among 2′-R-6'*H*-spiro(cycloalkyl-, heterocyclyl)–[1,2,4]triazolo[1,5-*c*]quinazolines.

Hence, to address above-mentioned challenges in treating cognitive and behavioral disorders following ketamine anesthesia, we employed a comprehensive research strategy combining computational design, organic synthesis, and biological evaluation.

Our approach focused on developing novel spiro(cycloalkyl-, heterocyclyl)[1,2,4]triazolo[1,5-*c*]quinazolines with improved target engagement profiles and reduced side effects compared to existing agents. The comprehensive methodological approach enabled systematic investigation of our novel compounds from molecular design through behavioral and neurobiochemical evaluation. In the following sections, we present the results of these studies, beginning with *in silico* computational analyses and progressing to *in vivo* efficacy and mechanism evaluations.

2. Results and Discussion

2.1. In Silico Analysis of Nootropic Potential

The main target for assessing the nootropic potential of the developed compounds was chosen glutamate receptor GluA3 (RCSB ID: 3LSX), due to its established role in the mechanisms of

 doi:10.20944/preprints202504.0388.v1

improving cognitive functions [43]. This ionotropic receptor mediates rapid excitatory synaptic transmission in the central nervous system and plays crucial roles in synaptic plasticity, learning, and memory processes. The selection of GluA3 as a target is particularly relevant given its involvement in cognitive enhancement pathways and its well-characterized structural interactions with established nootropics like piracetam [29,43]. Additionally, this receptor's role in neuroplasticity and potential therapeutic applications makes it an attractive target for novel cognitive enhancers [44].

The binding interactions were analyzed using the CB-Dock2 methodology for protein-ligand blind docking, incorporating cavity detection and homologous template fitting as described by Liu *et al.* [45] (Figure 3, Supplementary Materials, Table S1).

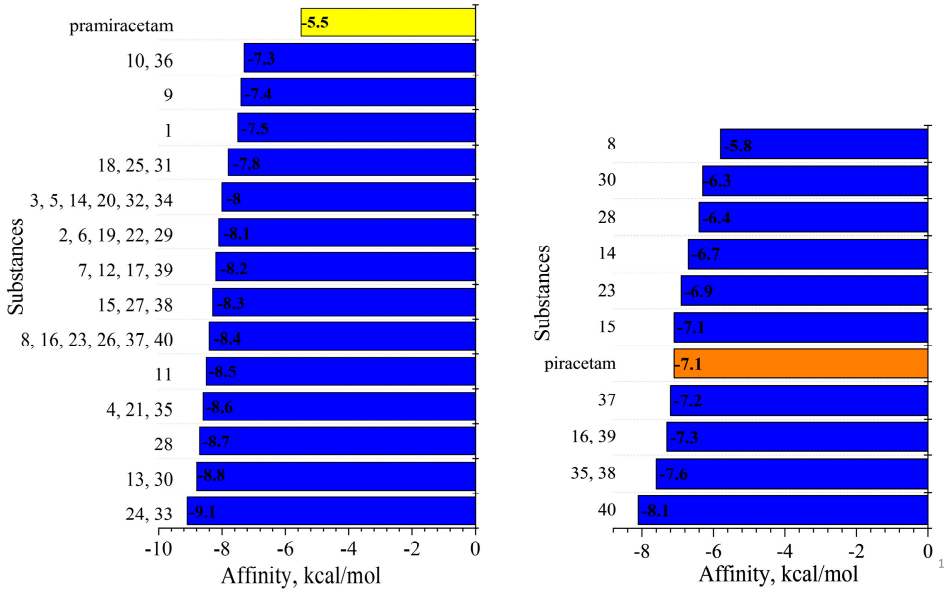

Figure 3. Comparative binding affinities of designed compounds to glutamate receptor 3 (GluA3) crystal structure (RCSB PDB ID: 3LSX). Left panel: Pramiracetam binding pocket (cavity volume: 126 Å³; center coordinates: -5, 22, 19; docking dimensions: 17 × 17 × 17 Å). Right panel: Piracetam binding pocket (cavity volume: 507 Å³; center coordinates: -12, 14, 21; docking dimensions: 19 × 19 × 19 Å).

Molecular docking analysis revealed, that 13 compounds of 40 demonstrated binding affinities exceeding 7.3 kcal/mol within the GluA3 active pocket, surpassing the reference compound piracetam serving as a reference compound, that exhibited relatively weak binding affinity (-5.5 kcal/mol). This observation aligns with established structural studies of α-amino-3-hydroxy-5-methyl-4-isoxazolepropionic acid (AMPA) receptor interactions, particularly the work of Ahmed and Oswald [43], who demonstrated that related racetam compounds interact through distinct allosteric binding sites. AMPA receptors are tetramers composed of combinations of four subunits (GluA1-GluA4), which can assemble in various combinations to form functional channels.

The found modest binding affinity is consistent with recent systematic reviews of racetam efficacy by Gouhie *et al.* [29], which found variable cognitive enhancement outcomes in clinical settings, suggesting that direct GluA3 interaction may not be the primary mechanism of action. This mechanistic complexity is further supported by recent analyses of nootropic compounds that highlight the diverse molecular pathways involved in cognitive enhancement [46]. Moreover, the comprehensive review by Jędrejko and colleagues also revealed that nootropic compounds can act through multiple mechanisms, including modulation of neurotransmitter systems, enhancement of neuronal metabolism, improvement of cerebral blood flow, and influence on neuroplasticity pathways.

So, the majority of synthesized compounds demonstrated binding affinities exceeding -8.0 kcal/mol against the target receptor, suggesting significant nootropic potential. Among which compounds **24** and **33** (-9.1 kcal/mol) show the strongest binding. Compound **24** is 2'-(pyridin-3-yl)-

 doi:10.20944/preprints202504.0388.v1

6'*H*-spiro[cyclohexane-1,5'-[1,2,4]triazolo[1,5-*c*]quinazoline], while **33** is 2'-(adamantan-1-yl)-1-methyl-6'*H*-spiro[piperidine-4,5'-[1,2,4]triazolo[1,5-*c*]quinazoline]. Compounds **13**, **30**, **28**, **4**, **21**, **35** features preferably heterocyclic rings like benzofuran, furan, and thiophene, and show high-medium affinity (-8.8 to -8.5 kcal/mol). Medium affinity (-8.4 to -8.0 kcal/mol) is shown by group of compounds including **11**, **8**, **16**, **23**, **26**, **37**, and **40**, etc. bearing various substituents at R position. Lower affinity (below -8.0 kcal/mol) notably includes compounds **1**, **9**, **10**, and **36** with smaller ring systems.

Moreover, the recent analysis of spiro[1,5'/4,5'-[1,2,4]triazolo[1,5-*c*]quinazoline] derivatives and their interaction with α1/β3/γ2L GABA(A) receptors (RCSB PDB ID: 6HUP) revealed important structure-activity relationships (Table S2) [47]. Our findings indicate that an optimal balance between structural rigidity and conformational flexibility appears essential for maintaining effective binding interactions. Compounds containing expanded ring systems exhibited enhanced binding affinity, with calculated binding energies ranging from -12.4 to -11.8 kcal/mol. The strategic positioning of hydrogen bond donors and acceptors within these molecular structures contributed significantly to specific receptor interactions. Interestingly, the incorporation of electron-rich heterocyclic systems, particularly furan and thiophene moieties, generally resulted in diminished binding affinity, likely due to unfavorable electronic distribution patterns that disrupted optimal ligand-receptor interactions.

So, the promising molecular docking results provided a strong rationale for proceeding with the synthesis of these compounds. Our synthetic efforts successfully delivered the target molecules in good to excellent yields, enabling further characterization and biological evaluation. However, *in vivo* experimental validation would be crucial to confirm cognitive enhancement effects, evaluate side effect profiles, determine optimal dosing and administration, and assess long-term safety and efficacy.

2.2. Synthesis

One of the approaches for constructing spiro derivatives is the [5+1]-cyclocondensation reactions, based on the interaction of 1,5-binucleophiles with carbonyl compounds [41]. Similarly, spiro[1,2,4]triazoloquinazolines (**1**-**40**) were obtained, specifically through the interaction of [2-(3-R-1*H*-1,2,4-triazol-5-yl)phenyl]amines (**a**) with cycloalkanones (cyclobutanone, cyclopentanone, cyclohexanone, 4-*tert*-butylcyclohexanone) or *N*-methylpiperidone (Figure 4).

The cyclocondensation proceeded without peculiarities in propan-2-ol in the presence of a catalytic amount of sulfuric acid, following a mechanism that included three main processes: carbinolamine formation, elimination of a water molecule, and intramolecular cyclization [48]. The target products are formed with satisfactory and high yields (67-95%) (Supplementary Materials, Spectral data). Furthermore, the reaction also proceeds in other organic solvents that are miscible with water and indifferent to the starting amines.

 doi:10.20944/preprints202504.0388.v1

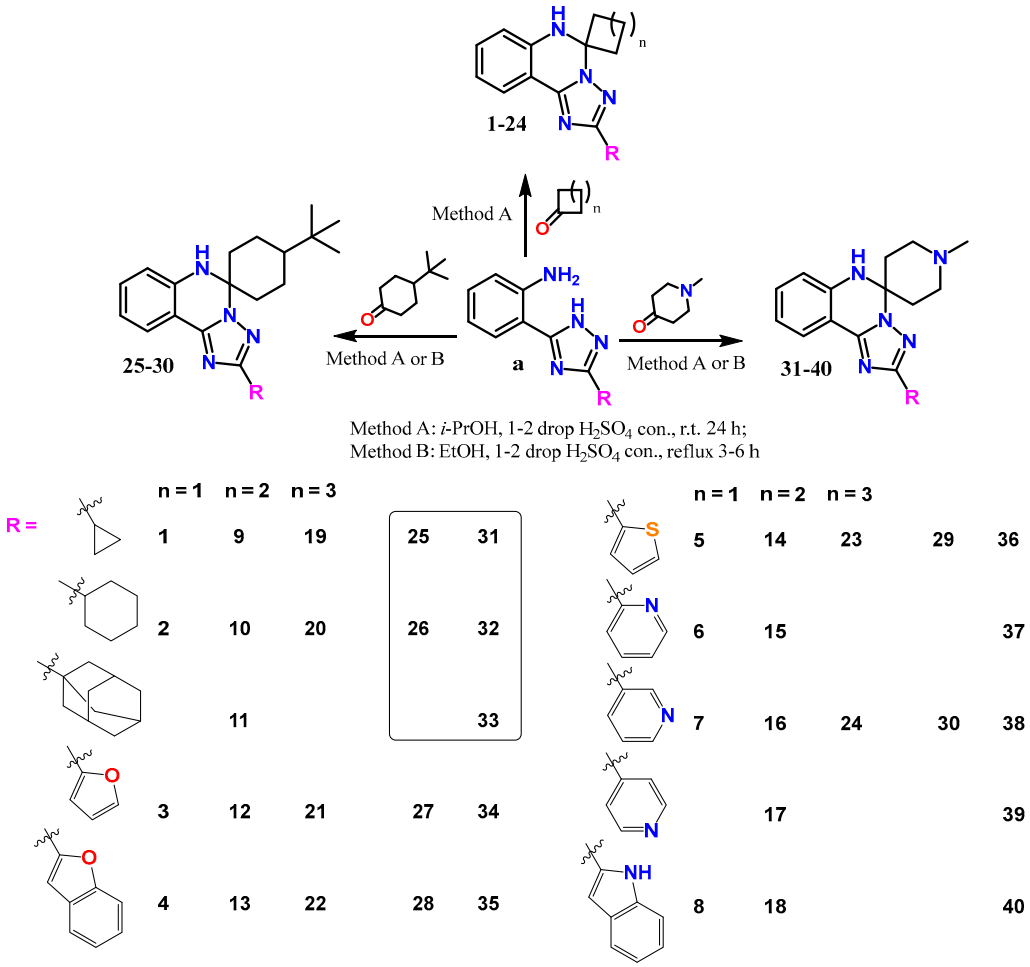

Figure 4. Synthetic route to 2′-R-6′*H*-spiro(cycloalkyl-, heterocyclyl)[1,2,4]triazolo[1,5-*c*]quinazolines (**1**-**40**) *via* acid-catalyzed condensation. Substances in the frame are chosen for *in vivo* studies.

The formation of compounds **1**-**40** was confirmed by chromatography-mass spectrometry, ^{1}H and ^{13}C NMR spectra, and elemental analysis. In the ^{1}H NMR spectra, the aromatic protons of the heterocycle form a characteristic ABCD system, which is represented by two doublets (H-7, H-9) and two triplets (H-8, H-10) with corresponding chemical shifts [41]. The characteristic proton of the NH-group (position 6) for these compounds is observed in the spectrum as a singlet in a wide range (7.22-3.79 ppm), and its chemical shift is determined by the donor-acceptor properties of the substituents in positions **2** and **5**. In some compounds, the signal of this proton is absent or resonates together with the aromatic protons of the quinazoline cycle. The proton signals of the spiro-condensed fragment in position 6′ and the substituent in position 2 of compounds **1**-**40** in most cases are easily interpreted and have classical shifts and multiplicity [49]. The ^{13}C NMR spectra of compounds additionally confirm the regioselective course of the [5+1]cyclocondensation reaction. Thus, the characteristic signals of the sp^{3}-hybridized Carbon atom in position 1,5′ were observed at 83.1-70.0 ppm.

Following successful synthesis and structural confirmation of compounds **1**-**40**, we proceeded to evaluate their safety profiles through comprehensive toxicity prediction studies. This critical step in our investigation aimed to identify compounds with optimal therapeutic indices for subsequent biological evaluation.

2.3. In Silico ADMET Studies

For *in vivo* study, we selected 5 compounds: **25**, **26**, **31**-**33**. The selection represents distinct structural variations (different R-groups or spiro-cyclic/heterocyclic systems) to explore structure-activity relationship of activity: spiro-junction of cyclohexane *vs.* *N*-methylpiperidine; 2'-position

 doi:10.20944/preprints202504.0388.v1

substituent: cyclopropyl *vs.* cyclohexyl *vs.* adamantyl; additional substituents: *tert*-butyl group in compounds **25** and **26**. Besides these compounds show consistently low toxicity predictions across multiple parameters [50] compared to other compounds in the series (Table 2). ProTox-II [51] and SwissADME analysis [52] were conducted to determine their compliance with toxicity and drug-likeness criteria. The results of the toxicity study showed that these compounds, like piracetam and fabomotizole that were chosen as references for further *in vivo* studies, belong to toxicity class IV. All compounds are distinctive for showing "no" predictions for all toxicity parameters evaluated, indicating a potentially safer pharmacological profile. Still, cytotoxicity is predicted for all mentioned substances, except **25** and **26**.

Table 2. Predicted toxicity of the compounds selected for the study *in vivo.*

Sub.	Toxicity index*	LD_{50}, mg/kg	Pred. acc., %	HT**	CG	IT	MG	CT
25	IV	2000	54.26	0.63	0.50	0.92	0.59	0.53
26		2000		0.65	0.50	0.95	0.61	0.53
31		1200		0.73	0.50	0.96	0.57	0.60/yes
32		2000		0.76	0.53	0.97	0.61	0.60/yes
33		1200		0.76	0.53	0.99	0.61	0.60/yes
fabomotizole		677		0.62	0.53	0.85	0.65	0.59/yes
piracetam		2000	100	0.95	0.61	0.99	0.84	0.62/yes

*Class IV: harmful if swallowed ($300 < LD_{50} \leq 2000$). Pred. acc.: prediction accuracy. Toxicity parameters measured on a 0-1 scale with higher values indicating greater potential toxicity: HT: Hepatotoxicity; CG: Carcinogenicity; IT: Immunotoxicity; MG: Mutagenicity; CT: Cytotoxicity (yes indicate potential cytotoxic effect).

While toxicity assessment provided valuable safety data, understanding the pharmacokinetic behavior of these compounds was equally important for their potential development as therapeutic agents. Therefore, we next examined their drug-likeness parameters and predicted ADME profiles to identify candidates with optimal bioavailability and blood-brain barrier penetration (Table 3) [50].

Hence, most of the studied compounds, like the reference drugs, meet the criteria for drug-likeness: MW (Da) (< 500), n-HBA (< 10), n-HBD (≤ 5), TPSA (< 140 Å²) and logP (≤ 5). The satisfactory TPSA value (> 140 Å²) for all compounds also correlates well with passive molecular transport across membranes. That is, the studied compounds will have a high ability to penetrate the blood-brain barrier and flexibly interact with molecular targets. Additionally, the studied compounds show high predicted bioavailability. An exception to these criteria is compound **26**, which has a high lipophilicity value (logP = 5.14), which can also be a positive characteristic, taking into account the structure of the neuron membrane. Importantly, the studied compounds pass the "drug-likeness" criteria for all filters (Lipinski, Veber, Muegge, Ghose, Egan), which are widely used in drug design. Only compound **25** and **26** piracetam have few violations of Veber and Egan filters.

 doi:10.20944/preprints202504.0388.v1

Table 3. Physicochemical descriptors and pharmacokinetic properties of chosen compounds provided by SwissADME.

Descriptors and properties	Compounds						
	25	**26**	**31**	**32**	**33**	**piracetam**	**fabomotizole**
MW (Da)	336.47	378.55	295.38	337.46	389.54	142.16	307.41
n-ROTB	2	2	1	1	1	2	6
n-HBA	2	2	3	3	3	4	4
n-HBD	1	1	1	1	1	6	1
TPSA	42.74	42.74	45.98	45.98	45.98	63.40	75.68
Consensus	4.21	5.14	2.20	3.16	3.71	-0.64	2.30
Molar refractivity	105.28	119.70	93.12	107.54	122.42	38.76	88.93
Gastrointestinal absorption	high						
Blood–brain barrier permeation			yes			no	yes
Drug likeness							
Lipinski (Pfizer); Muegge (Bayer); Ghose rules	yes						
Veber (GSK) rules			yes			no/ MW<160, WLOGP<-0.4, MR<40	yes
Egan filter	no/ XLOGP3>5			yes		no/MW<200	yes
Lead-likeness	no			yes		no	yes
Bioavailability Score	0.55						
Brenk alert, PAINS	no alerts						

* MW: Molecular weight; n-ROTB: number of rotatable bonds; n-HBA: number of Hydrogen bond acceptors; n-HBD: number of Hydrogen bond donors; TPSA: topological polar surface area; logP: octanol-water partition coefficient. "Yes" indicates the compound meets all criteria for the specified rule; "no" followed by specific parameters indicates which criteria were not met. Lipinski's Rule of Five states that an orally active drug generally has no more than one violation of the following criteria: MW ≤ 500 Da, logP ≤ 5, n-HBD ≤ 5, and n-HBA ≤ 10. Compounds violating more than one of these parameters are predicted to have poor absorption or permeation. Muegge (Bayer) rules evaluate drug-likeness based on the following parameters: MW: 200-600 Da; logP: -2 to 5; TPSA: ≤ 150 Å²; n-ROTB: ≤ 15; n-HBD: ≤ 5; n-HBA: ≤ 10; number of rings: ≤ 7; number of carbons: > 4; number of heteroatoms: > 1. Ghose rules define drug-like molecules as those with: MW: 160-480 Da; logP: -0.4 to 5.6; molar refractivity: 40-130; total number of atoms: 20-70; n-HBD: ≤ 5; n-HBA: ≤ 10. Egan filter evaluates compounds based on TPSA and WLOGP to predict passive intestinal absorption. Compounds with TPSA > 131.6 Å² and WLOGP > 5.88 are predicted to have poor absorption. Veber (GSK) rules: compounds are considered drug-like when they have ≤ 10 rotatable bonds and TPSA ≤ 140 Å². Brenk filter identifies structural fragments

 doi:10.20944/preprints202504.0388.v1

that may cause undesired reactivity, toxicity, or poor metabolic properties. PAINS (Pan-Assay Interference Compounds) filter identifies substructures that frequently cause false positives in high-throughput screening assays. "No alerts" alerts indicates compounds passed all criteria for the specified filter. The bioavailability score represents the probability of a compound having at least 10% oral bioavailability in rats or measurable Caco-2 permeability.

Moreover, all compounds in this study were evaluated against Brenk structural filters and Pan-Assay Interference compounds (PAINS) criteria. No structural alerts were identified, suggesting a reduced likelihood of false positives or reactive functionalities in the tested chemical series. However, absence of these alerts does not guarantee lack of other potential mechanisms of interference, and standard validation protocols were still employed.

In comparison to reference drugs included in the analysis (piracetam and fabomotizole), the novel spiro[1,2,4]triazolo[1,5-*c*]quinazoline derivatives exhibited generally higher molecular weights and aromaticity, but comparable or lower rotatable bond counts and polar surface areas.

Notably, fabomotizole contained significantly more rotatable bonds (6) than any of the novel compounds (1-2), suggesting the designed derivatives may benefit from reduced conformational entropy penalties upon binding. Piracetam, a marketed nootropic drug included as a reference, failed to meet several Ghose criteria due to its small size (MW < 160) and low lipophilicity (WLOGP < -0.4). This observation suggests that compounds with minor violations may still represent viable drug candidates, particularly when strong target engagement is demonstrated. As well as marketed drugs do not always conform to all druggability filters, particularly those with unique physicochemical properties or specific mechanisms of action.

Also, interestingly, that reference compounds demonstrated markedly different solubility profiles. Piracetam exhibited exceptional water solubility across all three models (classified as "highly soluble" by ESOL and Ali), consistent with its low molecular weight and hydrophilic character. Fabomotizole showed moderate solubility comparable to many of the novel derivatives, supporting the potential pharmaceutical viability of compounds with similar solubility profiles. Latter also demonstrated BBB penetration. And piracetam, as expected from its highly hydrophilic nature, showed no BBB penetration, consistent with its well-established favorable safety profile, but limited brain exposure.

Based on the favorable safety and pharmacokinetic profiles identified through *in silico* analyses, selected five representative compounds (**25**, **26**, **31-33**) were approved for in-depth biological evaluation. These compounds were chosen to represent key low toxic structural variations within our library, allowing for meaningful structure-activity relationship determinations in physiologically relevant models.

2.4. In Silico Analysis of Nootropic Potential

2.4.1. Open Field Test Following Ketamine Anesthesia

The ketamine-induced cognitive impairment paradigm was selected as the primary screening model for evaluating novel nootropic compounds [53–55]. This model demonstrates particular relevance for our structure-based approach due to the overlapping mechanisms between our target compounds and ketamine in glutamatergic and monoaminergic systems. The ketamine model offers several advantages for evaluating novel compounds. First, ketamine's well-characterized antagonism of NMDA receptors produces reproducible cognitive deficits that can be quantitatively measured. Second, these deficits share neurochemical similarities with a variety of clinical conditions where cognitive improvement is desired. Third, the model allows us to assess both direct cognitive enhancement and the ability to reverse the induced deficit, providing additional insights into the mechanisms of action of our compounds. Furthermore, this model is particularly relevant for the evaluation of compounds structurally related to reference molecules in our study, as these agents

 doi:10.20944/preprints202504.0388.v1

often act through glutamate-dependent mechanisms. Thus, the ketamine model provides a mechanistically relevant framework for evaluating our structural approach to drug development.

So, analysis of specific behavioral indicators in the open field test revealed that ketamine anesthesia significantly altered the behavioral characteristics of experimental animals (Table S3, Figure 5). Administration of ketamine (control group) led to a significant increase in total motor activity (48862.22±3612.2 cm²/s *vs.* 24175.01±2839.76 cm²/s in intact animals) and distance traveled by animals two days post-anesthesia (Table S3, Figure 5). Notably, free distance increased both in absolute units (604.8±32.71 cm *vs.* 59.37±26.31 cm in intact animals) and as a percentage of total motor activity (11.43±1% *vs.* 1.43±0.61%), representing an approximately 10-fold increase. Significant aggression was observed in animals two days after anesthesia. Additionally, the control group exhibited a 1.86-fold increase in freezing episodes (529±27 *vs.* 284±35 units) and a 1.5-fold increase in immobility (429±27 *vs.* 284±35 units). These behavioral changes collectively indicate the development of anxiety and heightened excitability in animals following ketamine anesthesia.

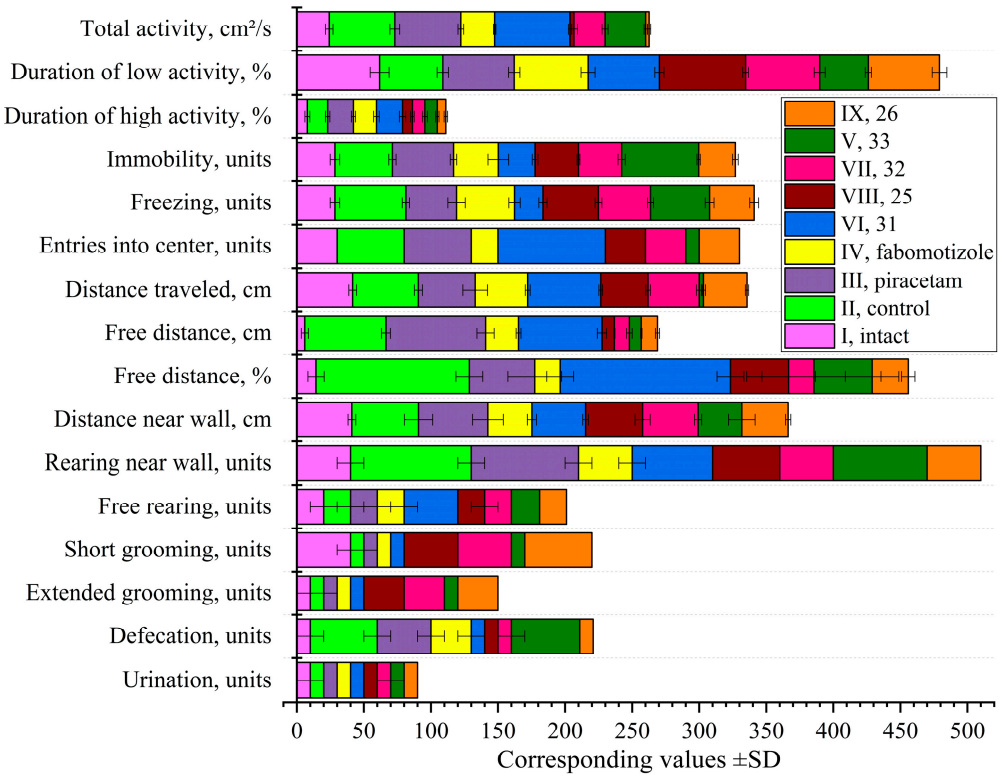

Figure 5. Comparative behavioral profile of experimental compounds on locomotor activity, exploratory behavior, and anxiety-like responses in the Open Field test following ketamine anesthesia. Data presented as normalized values (±SD) in ascending order of their sum for each studied compound from **26** to **31**. Data normalized for scale compatibility: total activity (cm²/s) divided by 1000; distance traveled and near wall distance (cm) divided by 100; immobility, freezing (units), and free distance (cm) divided by 10; free distance (%), number of entries into center, rearing near wall, free rearing, short grooming, extended grooming, defecation, urination (units) multiplied by 10. Significant differences ($p<0.05$) are found between treatment groups and either intact or control animals.

Ketamine administration did not affect the number of free rearings, but significantly increased rearings near the wall by 2.25-fold (9±1 *vs.* 4±1 units). Furthermore, the frequency of short grooming acts decreased by 4-fold (1±1 *vs.* 4±1 units) while extended grooming remained unchanged. These observations further support increased anxiety, excitability, and diminished comfort in ketamine-treated animals. The control group also demonstrated a 2-fold increase in high activity duration (15.12±1.63% *vs.* 7.83±1.87%), indicating elevated emotionality and excitability. This increased high

 doi:10.20944/preprints202504.0388.v1

activity can be interpreted as reduced efficiency in exploratory and search behaviors, as animals perform excessive "unnecessary" movements and require more time to adapt to novel environments.

Regarding the reference compounds, piracetam administration increased free distance compared to both intact and control groups (743.3±64.21 cm), but failed to reduce freezing episodes (378±65 units) or immobility (455±24 units), both remaining significantly higher than intact values. The number of wall rearings under piracetam remained elevated compared to the intact group (8±1 *vs.* 4±1 units), while short grooming acts remained at the control level (lower than intact values), and defecation frequency remained elevated (4±1 *vs.* 1±1 units in intact animals). These observations suggest that piracetam not only failed to reduce anxiety and fear following ketamine anesthesia but potentially exacerbated these states and the associated discomfort.

In contrast, fabomotizole significantly reduced free distance compared to control (245.32±18.23 cm *vs.* 604.8±32.71 cm), normalized immobility (334±77 units), and modestly reduced freezing episodes (432±42 *vs.* 529±27 units), though the latter remained significantly higher than intact values. However, fabomotizole did not normalize wall rearings, had minimal effects on high and low activity durations, and did not affect grooming behavior. These data indicate that fabomotizole partially reduces anxiety and fear after ketamine anesthesia but has limited impact on animal discomfort and cognitive activity.

Administration of tested compound in 10 mg/kg, namely **33** led to significant reductions in overall activity compared to the control group, though still elevated above intact levels (30321.33±1244.3 cm²/s). This group exhibited a pronounced alteration in activity structure, with a significant increase in immobility episodes (574±121 units). Compound **33** did not significantly reduce distance traveled but did decrease both high activity (9.33±1.22% *vs.* 15.12±1.63% in control) and low activity (36.21±2.33% *vs.* 47.11±4.22% in control and 61.71±7.08% in intact) durations. Animals displayed low mobility and preference for dark corners during testing, suggesting suppression of exploratory and cognitive activities. The number of center entries decreased (1 *vs.* 5 in control), potentially indicating either suppressed cognitive activity or persistent anxiety, despite reduced freezing episodes compared to control.

Compound **31** effectively reduced aggression following ketamine anesthesia while promoting active exploratory behavior. Animals receiving this compound showed significantly increased total activity compared to both control and intact groups (56177.4±1276.8 cm²/s). High activity duration was significantly increased (19.4±2.33%), suggesting enhanced cognitive engagement. The increased number of center entries (8 *vs.* 5 in control) and free rearings (4±1 *vs.* 2±1 units) further support improved exploratory behavior. However, the elevated free distance (622.3±34.3 cm), particularly in the context of increased high activity, may indicate somewhat inefficient exploratory patterns with excessive movements. Importantly, compound **31** significantly reduced anxiety markers, as evidenced by decreased freezing episodes (212±31 *vs.* 529±27 units), reduced immobility (274±21 *vs.* 429±27 units), increased center entries, and reduced defecation (1±1 *vs.* 5±1 units). These findings suggest a potential disinhibitory effect of compound **31.**

Compounds **25**, **26**, and **32** demonstrated particularly favorable behavioral profiles. All three compounds effectively reduced post-ketamine aggression while normalizing total activity to near-intact levels. Each compound significantly normalized high activity duration compared to control, while compound **25** additionally increased low activity duration (64.22±2.12% *vs.* 47.11±4.22% in control), suggesting enhanced quality of exploratory and cognitive behaviors. All three compounds significantly reduced freezing episodes and immobility, indicating anxiolytic effects.

Notably, compounds **25**, **26**, and **32** significantly reduced free distance, suggesting improved efficiency of exploratory activity. The number of center entries normalized to intact levels (3 entries), further supporting normalized cognitive function. Animals receiving these compounds also exhibited significantly increased short (4±1, 4±1, and 5±1 units, respectively, *vs.* 1±1 in control) and extended grooming (3±1 units for all three *vs.* 1±1 in control), along with decreased defecation (1±1 units for all three *vs.* 5±1 in control), indicating reduced anxiety and aggression alongside increased comfort.

 doi:10.20944/preprints202504.0388.v1

In summary, the behavioral analysis in the open field test following ketamine anesthesia revealed that compounds **25**, **26**, and **32** exhibited the most favorable profiles among all tested substances. These compounds effectively normalized behavioral parameters disrupted by ketamine, reducing anxiety and improving cognitive function without causing excessive stimulation or sedation.

Compound **31** demonstrated potent anxiolytic and stimulatory effects but may promote somewhat inefficient exploratory behavior. Compound **33** showed mixed effects with some anxiolytic properties but potential cognitive suppression. The reference compounds piracetam and fabomotizole exhibited limited efficacy, with piracetam potentially exacerbating certain anxiety parameters and fabomotizole showing only partial anxiolytic effects.

2.4.2. Study of Markers of Neuronal Damage

The experimental data presented in Figure 6 (Tables S4 and S5) provide valuable insights into the neurobiochemical changes induced by ketamine anesthesia and the potential neuroprotective effects of chosen two representatives, compounds **31** and **26**, compared to the reference drug piracetam.

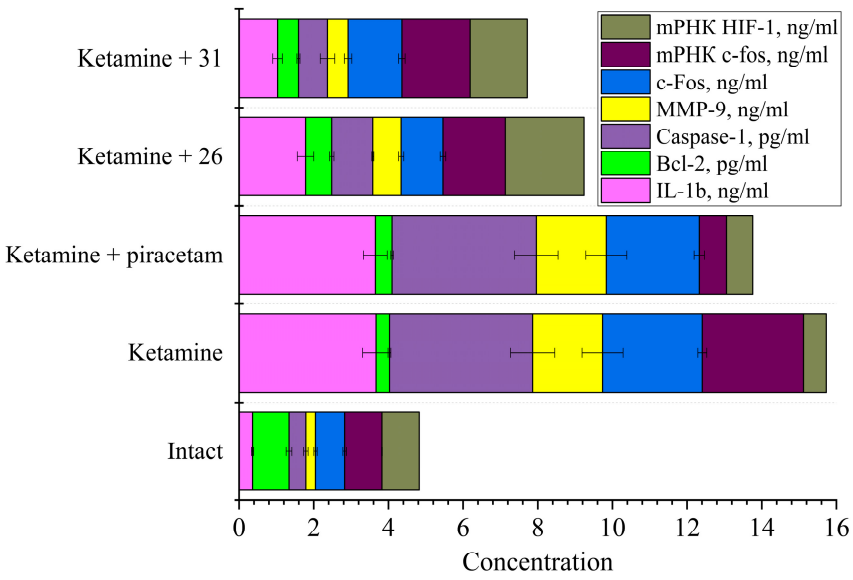

Figure 6. Neuroprotective effects of compounds on molecular markers and gene expression in rat brain following ketamine anesthesia. Effects on caspase-1 and Bcl-2 concentration in cytosolic fractions and on c-fos and HIF-1 mRNA expression in the CA1 hippocampal zone. Data for caspase-1 (pg/ml) and Bcl-2 (pg/ml) normalized by dividing by 100 for scale compatibility. Significant differences ($p<0.05$) compared to intact or control animals are indicated.

Inflammatory and apoptotic markers. Ketamine anesthesia significantly increased IL-1β concentration (approximately 11.8-fold) in the rat brain cytosolic fraction compared to intact animals. This substantial elevation indicates pronounced neuroinflammatory activation. Both compounds **31** and **26** demonstrated anti-inflammatory properties, reducing IL-1β levels by 72% and 51.5% respectively, compared to the control group. Notably, compound **31** showed superior anti-inflammatory efficacy. In contrast, piracetam failed to mitigate ketamine-induced IL-1β elevation, suggesting its limited anti-inflammatory capacity in this model.

The anti-apoptotic protein Bcl-2 was markedly reduced (by 63.4%) following ketamine administration, indicating compromised neuroprotective mechanisms. Both test compounds partially restored Bcl-2 levels, with compound **26** demonstrating greater efficacy (96.2% increase from

 doi:10.20944/preprints202504.0388.v1

control) compared to compound **31** (56.6% increase). Piracetam showed modest Bcl-2 restoration (25.1% increase), substantially less effective than the test compounds.

Inflammasome activation. Caspase-1, a key component of the inflammasome complex and indicator of pyroptotic cell death, was dramatically increased (8.5-fold) by ketamine anesthesia (Figure 6). Compounds **31** and **26** significantly attenuated this elevation, reducing levels by 79.7% and 71.3% respectively, with compound **31** showing slightly superior efficacy. Piracetam showed no effect on caspase-1 levels, suggesting its inability to modulate inflammasome activation.

Matrix metalloproteinase and neuronal activation. MMP-9, associated with blood-brain barrier disruption and neuroinflammation, increased 7.2-fold following ketamine administration. Both test compounds reduced MMP-9 levels, though the reduction did not reach the intact animal baseline. Piracetam showed no effect on MMP-9 elevation.

The neuronal activation marker c-fos increased 3.4-fold with ketamine anesthesia. Compounds **31** and **26** reduced c-fos protein levels by 46.1% and 58.1% respectively, with compound **26** showing greater efficacy. Piracetam minimally affected c-fos protein levels.

Gene expression analysis. The mRNA expression data from the CA1 hippocampal region revealed interesting patterns. Ketamine increased c-fos mRNA expression 2.7-fold, consistent with the protein level findings. Compounds **31** and **26** partially normalized c-fos transcription, reducing it by 32.5% and 38.4% respectively. Interestingly, piracetam reduced c-fos mRNA below intact animal levels, suggesting potential transcriptional suppression, that did not translate to proportional protein reduction.

Hypoxia-inducible factor 1 (HIF-1) mRNA was reduced by 38.9% following ketamine administration, indicating impaired hypoxic adaptation. Both test compounds not only restored but significantly elevated HIF-1 mRNA levels above intact baselines. Compound **26** showed superior efficacy, increasing HIF-1 mRNA 3.5-fold compared to control. Piracetam showed minimal effect on its ketamine-induced reduction.

Comparative efficiency and mechanism implications. Overall, compounds **31** and **26** demonstrated substantial neuroprotective properties across multiple parameters compared to piracetam. Their efficacy profiles suggest following different mechanistic pathways.

Compound **31** showed superior anti-inflammatory and anti-inflammasome activity, suggesting potent modulation of innate immune responses in the brain. Compound **26** demonstrated stronger effects on anti-apoptotic protein restoration and HIF-1 expression, indicating potentially greater influence on cell survival pathways and hypoxic adaptation.

Piracetam showed limited efficacy across most parameters, with modest effects only on Bcl-2 levels and c-fos transcription, consistent with its known mild neuroprotective profile.

The differential regulation of HIF-1 by the test compounds is particularly noteworthy, as it suggests potential enhancement of adaptive hypoxic responses, that may confer broader neuroprotection beyond inflammatory modulation.

These findings should be considered within the context of several limitations. The acute nature of the model may not fully represent chronic ketamine exposure scenarios. Additionally, regional specificity beyond the CA1 hippocampal zone was not assessed. Future investigations should examine the dose-dependency of these effects and explore additional brain regions and cell-specific responses to better characterize the neuroprotective mechanisms of compounds **31** and **26**.

Nevertheless, our results are consistent with the scientific concept of CNS disruption following ketamine anesthesia. Ketamine-induced NMDA receptor hyperstimulation triggers excessive Ca^{2+} influx, initiating a cascade of pathological events including reactive oxygen species (ROS) formation, neuroinflammation, and neuroapoptosis [56,57]. This mechanism aligns with established literature demonstrating that ketamine anesthesia precipitates postoperative cognitive dysfunction (POCD), characterized by anxiety and cognitive impairments stemming from neuroapoptotic processes. Particularly compelling is the dose-dependent apoptotic neurodegeneration observed in immature mouse brains following ketamine exposure, suggesting developmental vulnerability to anesthetic neurotoxicity [58].

 doi:10.20944/preprints202504.0388.v1

The neuroapoptotic pathway appears intricately linked to ketamine-induced c-fos expression across multiple brain regions. While NMDA receptor antagonism represents ketamine's primary mechanism of action, our findings support that ketamine-induced expression is mediated through additional pathways, notably sigma receptors. The complex pathogenesis of apoptosis in the nervous system involves numerous signaling systems, with immediate early response genes (c-jun, c-fos) playing a critical role. The c-fos protein functions as a transcriptional regulator for multiple inducible genes, orchestrating cellular growth and differentiation processes, thereby serving as a recognized marker of neuronal activation [59].

Our previous investigations demonstrated a significant increase in c-fos-positive cell density within the CA1 hippocampal region following ketamine anesthesia [16]. The current findings of elevated c-fos mRNA expression in this region corroborate these observations and align with independent reports in the literature [60,61], establishing a consistent pattern of ketamine-induced neuronal activation in hippocampal structures critical for memory formation.

POCD pathophysiology extends beyond neuronal activation to include enhanced transcription and expression of proinflammatory cytokines TNF-α and IL-1β, alongside microglial activation within the hippocampus. This neuroinflammatory response likely contributes substantially to hippocampus-dependent memory impairment. Moreover, systemic inflammation appears to exacerbate cognitive dysfunction induced by surgical interventions [62], suggesting a bidirectional relationship between peripheral and central inflammatory processes.

A pivotal finding in our study concerns ketamine's enhancement of caspase-1 expression, which not only elevates TNF-α and IL-1β levels but also initiates pyroptosis - a distinct form of programmed cell death. Caspase-1-dependent pyroptosis emerges as a significant pathway involved in mitochondria-related apoptosis underlying ketamine-induced hippocampal neurotoxicity [63]. This mechanism may represent a critical convergence point between inflammatory and apoptotic processes in anesthetic-induced neurotoxicity.

Further exacerbating these pathological processes, ketamine-induced matrix metalloproteinase-9 (MMP-9) expression amplifies both neuroapoptosis and neuroinflammation, potentially through blood-brain barrier disruption [64]. Our compounds demonstrate efficacy in mitigating these neuroinflammatory effects associated with POCD and memory dysfunction.

The molecular basis of ketamine neurotoxicity further involves significant reduction in anti-apoptotic protein (Bcl-2) expression, increased pro-apoptotic protein Bax expression, and stimulated cytochrome-c release from mitochondria in primary cortical neurons [59]. Our investigation reveals that anesthetic-induced neuroapoptosis and cognitive dysfunction are associated with suppression of protective proteins HSP70 and HIF-1 expression [65], with decreased HIF-1 expression specifically documented in this study.

The neurobiochemical data presented above provides valuable mechanistic insights into the neuroprotective effects of our novel compounds. Ketamine anesthesia clearly induces a complex cascade of pathological events involving neuroinflammation, cell death pathways, and altered gene expression. Compounds **31** and **26** demonstrate distinct patterns of efficacy across these pathways, suggesting structure-dependent mechanisms of action. To better understand these structure-function relationships and inform future drug development efforts, we next conducted a comprehensive analysis of the structural features that drive the observed biological activities and efficacy profiles of compounds.

2.5. Structure-Activity Relationships

2.5.1. Correlation Molecular Structure and Behavioral Profiles

The results presented in the Table 4 reveal several found important structure-activity relationships among studied compounds in the post-ketamine anesthesia recovery model.

 doi:10.20944/preprints202504.0388.v1

Table 4. Structure-activity relationship of novel 6'*H*-spiro[cyclohexane/piperidine-1,5'/4,5'-[1,2,4]triazolo[1,5-*c*]quinazoline] derivatives in post-ketamine recovery model.

Sub.	Structural features	Behavioral profile	Key effects	Potential applications
25	spiro cyclohexane 2'-cyclopropyl 4-(*tert*-butyl)	Anti-hyperactivity	Normalized total activity Reduced high activity duration Increased low activity duration Normalized immobility Increased grooming behavior	Ketamine recovery Potential anxiolytic
26	spiro cyclohexane 2'-cyclohexyl 4-(*tert*-butyl)	Anti-hyperactivity	Normalized total activity Reduced high activity duration Normal low activity Reduced immobility Increased grooming behavior	Ketamine recovery Mild anxiolytic
31	spiro *N*-methylpiperidine 2'-cyclopropyl	Stimulatory / Anxiolytic	Increased total activity Increased high activity duration Maximum center entries Increased distance traveled High free distance	Anxiolytic Potential anti-depressant Enhanced recovery
32	spiro *N*-methylpiperidine 2'-cyclohexyl	Anti-hyperactivity	Normalized total activity Reduced high activity duration Normal low activity Increased grooming behavior	Ketamine recovery Anxiolytic
33	spiro *N*-methylpiperidine 2'-adamantyl	Sedative-like	Moderately reduced activity Minimal center entries Highest immobility Reduced distance traveled Maintained elevated defecation	Sedative Potential hypnotic Different mechanism than traditional anxiolytics

 doi:10.20944/preprints202504.0388.v1

Influence of the spiro-junction type

The spiro-junction (cyclohexane *vs. N*-methylpiperidine) appears to dictate not only behavioral outcomes but also specific neurobiochemical pathways:

Cyclohexane spiro-junction (compounds **25** and **26**) confers stabilizing effects on ketamine-induced behavioral alterations. Neurobiochemically, compound **26** demonstrated superior efficacy in Bcl-2 restoration and HIF-1 upregulation, suggesting that this structural element may preferentially modulate cell survival pathways and hypoxic adaptation mechanisms rather than direct anti-inflammatory actions.

N-methylpiperidine spiro-junction (compounds **31**, **32**, and **33**) yields diverse activity profiles that strongly depend on the 2'-substituent. The basic nitrogen atom in the piperidine ring may enhance compound **31**'s anti-inflammatory properties, as evidenced by its superior reduction of IL-1β and caspase-1 levels. This suggests that the *N*-methylpiperidine scaffold may facilitate interactions with inflammatory mediators or their regulatory pathways.

Impact of 2'-position substituents

The 2'-position substituent critically determines both behavioral and neurobiochemical profiles:

Cyclopropyl substitution: When combined with *N*-methylpiperidine (compound **31**), it produces stimulatory/anxiolytic effects behaviorally while demonstrating superior anti-inflammatory and anti-inflammasome activity. The compact, rigid cyclopropyl group may enhance binding to specific receptors or proteins involved in inflammatory cascades. In contrast, when paired with cyclohexane (compound **25**), it yields anti-hyperactivity effects, suggesting a complex interplay between this substituent and the spiro-junction type.

Cyclohexyl substitution: Derivatives with this moiety (compounds **26** and **32**) consistently normalize ketamine-induced hyperactivity regardless of the spiro-junction type. Notably, compound **26** demonstrated exceptional efficacy in restoring Bcl-2 levels and elevating HIF-1 mRNA expression, suggesting that the cyclohexyl group may optimize interactions with proteins involved in cell survival and hypoxic adaptation pathways.

Adamantyl substitution: The adamantyl-piperidine derivative (**33**) displays a unique sedative-like profile. While not directly examined in the neurobiochemical analyses, its structural properties suggest it may have distinct effects on neuronal signaling, possibly through enhanced blood-brain barrier penetration or interaction with sedation-mediating receptors.

2.5.2. Behavioral Markers and Neurobiochemical Correlates

Self-grooming behavior and neuroinflammation. Compounds **25**, **26**, and **32** significantly increased both short and extended grooming behaviors. Interestingly, compounds **26** and **31** (examined in the neurobiochemical analyses) both reduced IL-1β and caspase-1 levels, suggesting that attenuation of neuroinflammation might contribute to normalized grooming patterns. The differential effects on c-fos expression (with compound **26** showing greater reduction) may further explain the nuanced behavioral differences between these compounds.

Locomotor activity and HIF-1 expression. The normalization of locomotor activity observed with compound **26** correlates with its remarkable ability to upregulate HIF-1 mRNA. HIF-1 plays a critical role in neural adaptation to stress conditions, and its enhanced expression may contribute to improved behavioral recovery through optimized neuronal metabolism and resilience.

2.5.3. Structure-Based Optimization Strategies

Based on these integrated findings, we propose refined optimization strategies:

For anxiolytic compounds with anti-inflammatory properties, the cyclopropyl-piperidine scaffold (compound **31**) offers a promising starting point. Further modifications could enhance its anti-inflammatory potency while preserving its anxiolytic behavioral profile.

 doi:10.20944/preprints202504.0388.v1

For neuroprotective agents that normalize ketamine-induced hyperactivity, the cyclohexyl derivatives (compounds **26** and **32**) provide excellent lead structures. Optimization efforts could focus on enhancing Bcl-2 restoration and HIF-1 upregulation while maintaining their behavioral benefits.

For dual-action compounds targeting both inflammation and apoptosis, hybrid structures incorporating features from both compounds **31** and **26** could yield candidates with complementary mechanisms of action.

For sedative compounds, the adamantyl-piperidine structure (compound **33**) could be further optimized, with additional investigation of its neurobiochemical profile to understand its mechanism of action.

2.5.4. Molecular Mechanisms and Target Hypotheses

The differential effects on inflammatory markers (IL-1β, caspase-1), apoptotic regulators (Bcl-2), and adaptive response factors (HIF-1) suggest multiple molecular targets for these compounds:

Compound **31**'s superior anti-inflammatory and anti-inflammasome activity suggests potential interaction with inflammasome components (NLRP3, ASC) or upstream regulators. Compound **26**'s pronounced effect on Bcl-2 and HIF-1 suggests possible modulation of mitochondrial function or hypoxia-sensing pathways. The differential effects on MMP-9 and c-fos indicate that these compounds may also influence neuronal activation and matrix remodeling processes.

The interplay between glutamatergic and GABAergic neurotransmission critically influences cognitive behaviors affected by ketamine. Post-ketamine activation of specific GABAergic pathways beneficially impacts spontaneous motor behavior, environmental habituation, and spatial learning in experimental paradigms. This suggests a potential shift in GABAergic signaling from receptor-mediated effects toward neurometabolic functions, particularly energy metabolism and mitochondrial processes [22,66–68].

Our data align with findings that modulation of serotonergic signaling - specifically 5-HT1A receptor blockade coupled with 5-HT2A receptor activation - reduces hippocampal apoptosis and attenuates anxiety, motor impairments, and environmental habituation deficits induced by various pharmacological agents [69,70]. The novel compounds investigated here, possessing affinity for GABA and specific serotonin receptor subtypes, appear to interrupt the cascade of adverse molecular and biochemical reactions following ketamine administration. This interruption attenuates excitotoxicity, neuroinflammation, neuroapoptosis, and reduced endogenous neuroprotection, thereby mitigating subsequent anxiety, irritability, spontaneous behavior impairments, and learning and memory deficits.

The comprehensive neuroprotective profile of compounds **31** and **26** against multiple ketamine-induced pathological processes presents promising therapeutic potential for preventing or treating anesthetic-induced neurocognitive dysfunction. Their differential mechanistic actions on inflammatory, apoptotic, and adaptive pathways warrant further investigation in diverse anesthetic exposure paradigms and potential clinical translation.

Further receptor binding and mechanistic studies would help elucidate the precise molecular targets responsible for these effects. This integrated structure-activity relationship analysis provides a rational basis for the design of novel 2'-R-6'*H*-spiro(cycloalkyl, heterocyclyl)[1,2,4]triazolo[1,5-*c*]quinazolines with targeted effects on specific neurobiochemical pathways. The identified patterns could guide the development of new therapeutic agents for managing ketamine anesthesia recovery or treating neuroinflammatory and anxiety-related conditions.

2.6. In Silico Molecular Docking to Nootropic and Anxiolytic Targets

2.6.1. Molecular Docking General Results

Three representative compounds were selected for in-depth investigation based on their distinctive structural features and pharmacological profiles: compounds **24** (2'-(pyridin-3-yl)-6'*H*-spiro[cyclohexane-1,5'-[1,2,4]triazolo[1,5-*c*]quinazoline]), **26** (spiro cyclohexane with 2'-cyclohexyl

 doi:10.20944/preprints202504.0388.v1

substitution), and **31** (spiro *N*-methylpiperidine with 2'-cyclopropyl substitution). This selection encompasses compounds with demonstrated *in vivo* efficacy (**26** and **31**) and superior binding affinity to key receptors (**24**).

The following receptors represent major therapeutic targets across various neurological, psychiatric, and cardiovascular conditions, and were chosen as the targets. CB2 (5ZTY): Signal transduction and cell communication with roles in anxiety-like behaviors, particularly demonstrated in predator-induced fear models [34]. GABA(A)R α1/β3/γ2L (6HUP): Major inhibitory neurotransmitter receptor involved in anxiety regulation, sleep regulation, and sedation, particularly relevant for trauma-related disorders [71]. M2 muscarinic acetylcholine receptor (5ZKB): Involved in memory, attention, and varios physiological functions as characterized in structural studies [27]. D2 dopamine receptor (6CM4): Critical for reward, motor control, and executive function, with structural insights informing therapeutic development [36]. Serotonin 1A (5-HT1A) receptor (8FYX): Key role in anxiety and depression regulation, with demonstrated anxiolytic effects in amygdala [35]. Serotonin 7 (5-HT7) receptor (7XTC): Involved in mood regulation and cognitive processes, characterized through selective antagonist studies [30]. CRF1R (4K5Y): Central to stress response and anxiety behaviors, with established pharmacological profiles in stress-related disorders [33]. Glutamate receptor 3 (GluA3) (3XSL): These receptors mediate fast excitatory synaptic transmission in the brain by allowing the influx of cations (primarily sodium and calcium) upon binding of the neurotransmitter glutamate [43]. mGluR5 (4OO9): Critical for synaptic plasticity and learning, with structural insights informing therapeutic development [31].

The molecular docking analyses reveal remarkable binding profiles across multiple neuronal targets (Figure 7, Table S6), providing mechanistic insights into the neurobiochemical and behavioral effects observed in previous studies.

Additionally, compounds demonstrated significant binding capacities beyond primary reference sites towards 8FYX, 7XTC, 4K5Y and 4OO9 (Figure 7, left panel, Table S7-S14), that differ from the reference ones, and had higher affinity value. This indicates specific structural complementarity to the primary binding sites while retaining flexibility for alternative binding modes.

Compound **26***: balanced multi-target engagement and neuroprotection*

The molecular docking results for compound **26** demonstrate balanced binding across multiple targets, with particularly strong affinity for the M2 muscarinic acetylcholine receptor (5ZKB, -10.7 kcal/mol) and GABA(A) receptor (6HUP, -10.4 kcal/mol). This multi-target engagement profile correlates with its comprehensive neuroprotective effects observed in neurobiochemical studies:

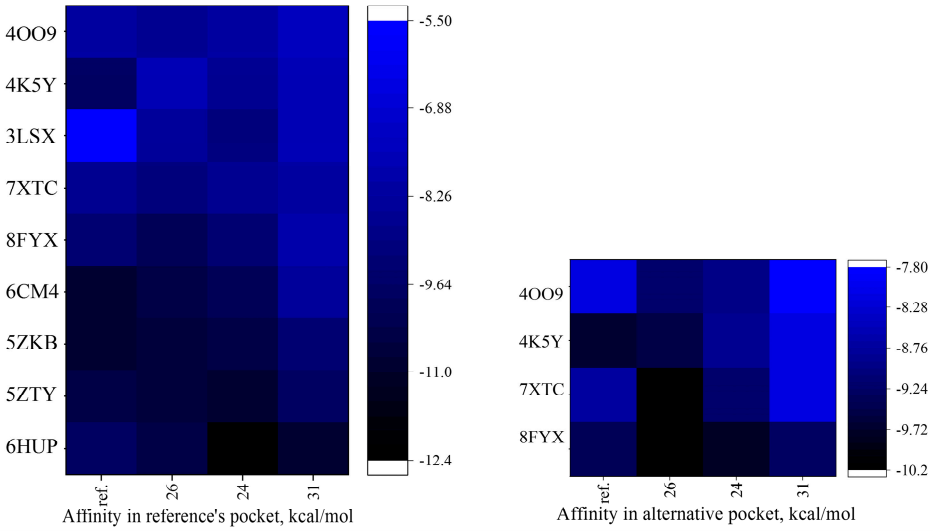

Figure 7. Binding affinities of compounds to nootropic and anxiolytic receptors. *Left panel*: Substance binding energies in reference's pocket (kcal/mol). *Right panel*: Substances best binding energies in alternative pockets

 doi:10.20944/preprints202504.0388.v1

(kcal/mol). Color intensity indicates binding strength (darker = stronger binding). Target receptors (RCSB PDB IDs) / reference substance: 6HUP: α1/β3/γ2L GABA(A)R / diazepam; 5ZTY: G protein coupled receptor / JWH-133; 5ZKB: M2 muscarinic acetylcholine receptor / AFDX-384; 6CM4: D2 dopamine receptor / risperidone; 8FYX: serotonin 1A (5-HT1A) receptor-Gi1 protein / buspirone; 7XTC: serotonin 7 (5-HT7) receptor-Gs-Nb35 / SB-269970; 3XSL: glutamate receptor 3 (GluA3) / pramiracetam; 4K5Y: corticotropin-releasing factor receptor 1 (CRF1R) / CP-154,526; 4OO9: human class C GPCR metabotropic glutamate receptor 5 transmembrane domain / mavoglurant.

M2 muscarinic receptor binding and cognitive effects: The strong binding to M2 muscarinic receptors may contribute to the compound's ability to normalize ketamine-induced hyperactivity without excessive sedation. This cholinergic modulation could enhance cognitive recovery, consistent with **26**'s ability to normalize total activity and reduce high activity duration in behavioral studies.

GABA(A) receptor modulation and anti-anxiety effects: The substantial affinity for GABA(A) receptors suggests anxiolytic properties, which align with the increased grooming behavior observed in behavioral studies—a marker of reduced anxiety in rodents.

Multi-target engagement and HIF-1 upregulation: The balanced binding profile across serotonergic (8FYX, 7XTC) and glutamatergic (3LSX, 4OO9) targets may underlie the compound's remarkable ability to upregulate HIF-1 mRNA expression (3.5-fold increase compared to control). This molecular signature suggests activation of multiple complementary signaling pathways that converge on adaptive stress responses.

Bcl-2 restoration and receptor profile: The exceptional efficacy in restoring Bcl-2 levels (96.2% increase from control) correlates with the compound's strong binding to cannabinoid receptors (5ZTY, -10.6 kcal/mol), which have been implicated in cell survival pathways.

Compound **31***: Selective anti-inflammatory activity despite lower overall binding*

Compound **31** consistently demonstrated lower binding affinities across most targets compared to compounds **24** and **26**. However, it exhibited remarkable anti-inflammatory and anxiolytic properties in neurobiochemical and behavioral studies. This apparent discrepancy provides important insights:

Moderate GABA(A) binding and anxiolytic effects: Despite lower binding affinity to GABA(A) receptors (6HUP, -10.8 kcal/mol) compared to compound **24**, compound **31** demonstrated pronounced anxiolytic-like effects behaviorally. This suggests its anxiolytic mechanism may involve pathways beyond direct GABA(A) modulation.

Anti-inflammatory prominence despite modest binding: Compound **31**'s superior anti-inflammatory properties (72% reduction in IL-1β levels) and potent anti-inflammasome activity (79.7% reduction in caspase-1) contrast with its more modest receptor binding profile. This suggests its primary mechanism may involve modulation of inflammatory signaling cascades downstream of receptor activation rather than direct receptor antagonism.

Stimulatory profile and receptor engagement: The stimulatory behavioral effects observed (increased high activity duration, maximum center entries) may relate to its moderate binding to dopamine D2 receptors (6CM4, -8.3 kcal/mol) and serotonin receptors, indicating a complex interplay between monoaminergic systems.

Compound **24***: Strong GABA(A) affinity with potential cognitive enhancement*

While not directly evaluated in the neurobiochemical and behavioral studies, the molecular docking results for compound **24** reveal exceptional binding to GABA(A) receptors (6HUP, -12.4 kcal/mol), substantially exceeding the reference compound diazepam (-9.8 kcal/mol):

Superior GABA(A) binding: The exceptionally strong GABA(A) receptor affinity suggests potentially potent anxiolytic or sedative effects that warrant future behavioral evaluation.

Glutamate receptor engagement: Strong binding to glutamate receptor 3 (GluA3, 3LSX, -9.1 kcal/mol) substantially exceeding the reference pramiracetam (-5.5 kcal/mol) suggests potential cognitive enhancement capabilities.

 doi:10.20944/preprints202504.0388.v1

Balanced multi-target profile: The strong binding across cannabinoid, muscarinic, and dopaminergic targets suggests a multi-modal mechanism of action that may provide cognitive enhancement without excessive sedation.

Following the quantitative assessment of binding affinities through molecular docking simulations, the three-dimensional visualization of protein-ligand complexes provides critical spatial insights not captured by numerical scores alone. These 3D representations elucidate key intermolecular interactions, including hydrogen bonding networks, hydrophobic contacts, and potential steric hindrances, thereby contextualizing the previously calculated binding energies within the framework of the binding pocket.

2.6.2. Structural Comparison and Binding Site Interactions

This comparative visualization (Figure 8) demonstrates how subtle structural modifications to the triazoloquinazoline scaffold produce distinct receptor binding profiles and subsequent pharmacological effects, providing molecular insights into their mechanism of action and therapeutic potential.

Panel A. The 2'-(pyridin-3-yl) derivative **24** demonstrates exceptional binding affinity (-12.4 kcal/mol) to the GABA(A) receptor, substantially exceeding the reference compound diazepam (-9.8 kcal/mol) [47]. This enhanced binding profile can be attributed to its diverse interaction network. The molecular interaction data reveals that compound **24** forms multiple hydrogen bonds with the receptor, including a strong conventional hydrogen bond with SER206 (3.09 Å), suggesting a key anchoring point for ligand recognition. Additionally, carbon hydrogen bonds with ASP56 and SER205 further stabilize the complex. The interaction profile is notably enriched by extensive hydrophobic contacts, particularly π-π stacked interactions with TYR58, TYR210, and PHE77. These aromatic interactions likely contribute significantly to the compound's high binding affinity by providing optimal spatial orientation within the binding pocket. The presence of both hydrogen bonding and hydrophobic interactions creates a complementary binding mechanism that explains the substantially higher affinity compared to diazepam.

Panel B. Compound **31**, the *N*-methylpiperidine spiro derivative with 2'-cyclopropyl substitution, displays moderate binding affinity (-10.8 kcal/mol) to the GABA(A) receptor, also exceeding the reference compound diazepam. Its interaction profile appears more selective, primarily featuring a π-donor hydrogen bond with SER205 (3.75 Å) and prominent π-π stacked hydrophobic interactions with PHE77 and TYR210.

The reduced number of interactions compared to compound **24** correlates with its moderately lower binding affinity, suggesting that the cyclopropyl moiety provides sufficient but not optimal receptor engagement. Notably, both compounds **24** and **31** interact with similar residues (SER205, PHE77, TYR210), indicating a common binding mode at the GABA(A) receptor despite their structural differences.

 doi:10.20944/preprints202504.0388.v1

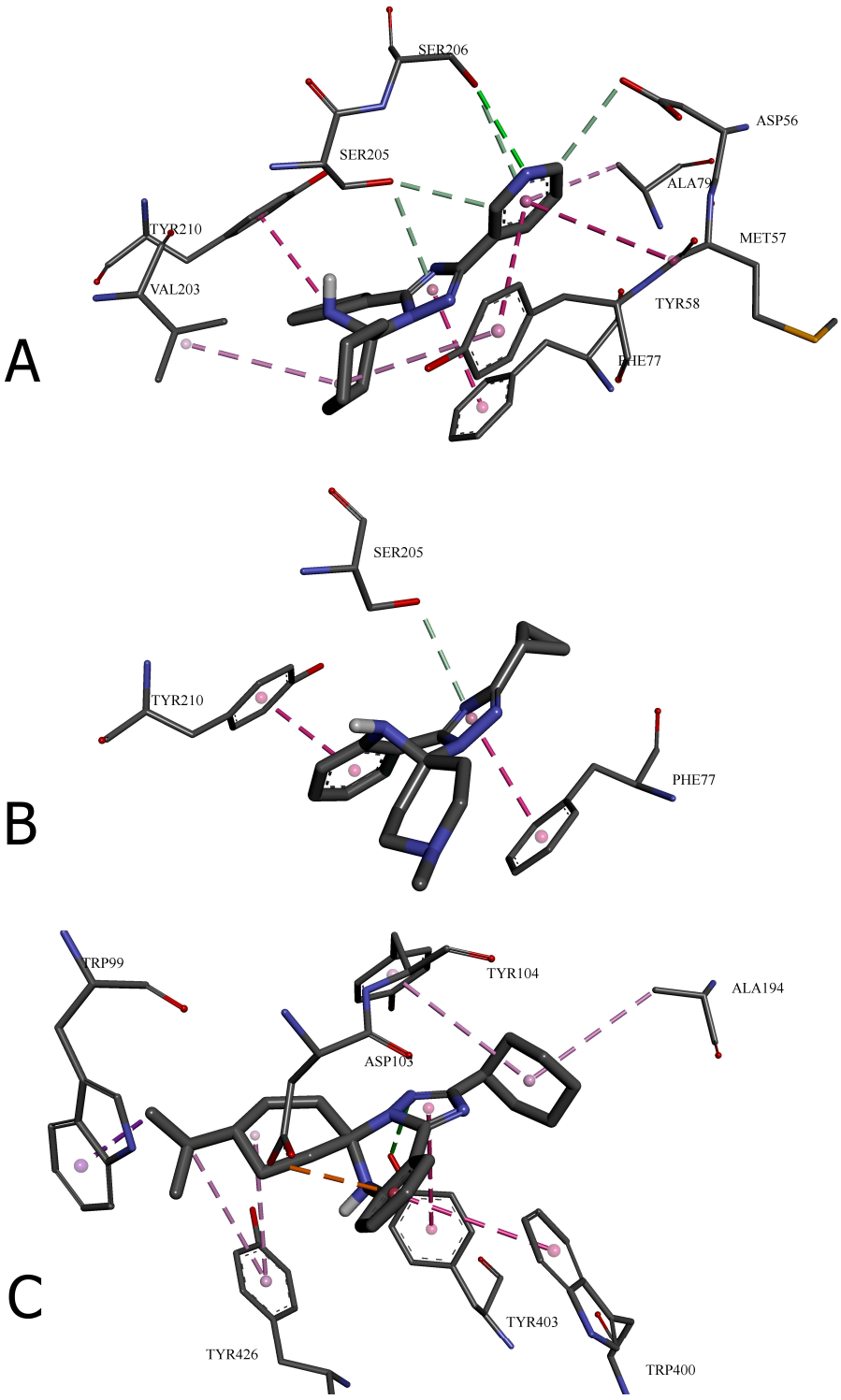

Figure 8. 3D visualization of molecular docking analyses of compounds **24**, **26**, and **31** with their primary receptor targets, highlighting different molecular interactions color-coded as follows: conventional hydrogen bonds (green), carbon hydrogen bonds and π-donor hydrogen bonds (light green), π-π stacked interactions, amide-π stacked and π-sigma interactions (purple), π-π T-shaped interactions (pink), alkyl, π-alkyl interactions (light pink), and electrostatic π-anion interactions (orange). *Panel A*. Compound **24** with GABA(A) receptor (PDB ID: 6HUP). *Panel B*. Compound **31** also with GABA(A) receptor (PDB ID: 6HUP). *Panel C*. Compound **26** with M2 muscarinic acetylcholine receptor (PDB ID: 5ZKB).

 doi:10.20944/preprints202504.0388.v1

Table 5. Molecular interactions between novel compounds (**24**, **31**, and **26**) and neurotransmitter receptors: bond distances, categories, and types.

Amino acid residue	Distance, Å[3]	Bond category	Bond type
24 with GABA(A) receptor (6HUP)			
SER206	3.09118	Hydrogen Bond	Conventional Hydrogen Bond
ASP56	3.2852	Hydrogen Bond	Carbon Hydrogen Bond
SER205	3.28938	Hydrogen Bond	Carbon Hydrogen Bond
SER205	3.67482	Hydrogen Bond	π-Donor Hydrogen Bond
SER206	3.90775	Hydrogen Bond	π-Donor Hydrogen Bond
TYR58	5.76264	Hydrophobic	π-π Stacked
TYR210	4.04531	Hydrophobic	π-π Stacked
PHE77	4.01868	Hydrophobic	π-π Stacked
MET57	5.04132	Hydrophobic	Amide-π Stacked
VAL203	4.58572	Hydrophobic	Alkyl
TYR58	4.9221	Hydrophobic	π-Alkyl
ALA79	4.92852	Hydrophobic	π-Alkyl
31 with GABA(A) receptor (6HUP)			
SER205	3.7526	Hydrogen Bond	π-Donor Hydrogen Bond
PHE77	3.96894	Hydrophobic	π-π Stacked
TYR210	3.99648	Hydrophobic	π-π Stacked
26 with M2 muscarinic acetylcholine receptor (5ZKB)			
TYR403	2.87801	Hydrogen Bond	Conventional Hydrogen Bond
ASP103	3.70202	Electrostatic	π-Anion
TRP99	3.93043	Hydrophobic	π-Sigma
TRP400	4.88215	Hydrophobic	π-π T-shaped
TYR403	5.0193	Hydrophobic	π-π T-shaped
ALA194	4.93091	Hydrophobic	Alkyl
TYR104	5.41339	Hydrophobic	π-Alkyl
TYR426	5.13581	Hydrophobic	π-Alkyl
TYR426	5.27219	Hydrophobic	π-Alkyl

* Bond distances are reported in Angstroms (Å) and represent the shortest atomic distance between the interacting groups. Smaller distances generally indicate stronger interactions, particularly for hydrogen bonds where distances below 3.0 Å typically represent strong binding. Hydrogen bonds are classified into conventional, carbon hydrogen, and π-donor types based on the interacting atoms and their geometrical orientation. Conventional hydrogen bonds typically involve electronegative atoms (O, N) as acceptors. Hydrophobic interactions are categorized as π-π stacked, π-π T-shaped, amide-π stacked, alkyl, and π-alkyl based on the relative orientation of aromatic rings and aliphatic groups. The electrostatic π-anion interaction observed between compound **26** and ASP103 of the M2 receptor involves negatively charged carboxylate groups interacting with the electron-rich π system of the ligand. These molecular interactions contribute to the binding affinity and specificity of the compounds for their respective receptors, potentially correlating with their pharmacological activities.

Panel C. Compound **26**, the 2'-cyclohexyl derivative, demonstrates strong binding (-10.7 kcal/mol) to the M2 muscarinic receptor, comparable to the reference antagonist AFDX-384 (-10.9 kcal/mol). Its interaction profile differs significantly from the GABA(A)-binding compounds, highlighting receptor selectivity among these derivatives.

 doi:10.20944/preprints202504.0388.v1

The strong conventional hydrogen bond with TYR403 (2.88 Å) appears to be a critical anchoring point for recognition at the M2 receptor. Uniquely, compound **26** exhibits an electrostatic π-anion interaction with ASP103, not observed with the other compounds. This electrostatic component likely contributes significantly to its binding specificity for the M2 receptor.

The hydrophobic interaction network is also distinctive, featuring π-sigma interaction with TRP99 and π-π T-shaped interactions with TRP400 and TYR403, instead of the π-π stacked interactions observed with GABA(A) receptor binders. The different geometrical orientation of these hydrophobic contacts suggests receptor-specific spatial accommodation of the cyclohexyl moiety.

The predominance of aromatic interactions across all compounds highlights the importance of the triazoloquinazoline core scaffold in receptor recognition.

2.6.3. Refined Structure-Activity Relationships

Integration of molecular docking results with previous neurobiochemical and behavioral findings reveals comprehensive structure-activity relationships:

Spirocyclic core determinants

Cyclohexane-based spirocycles (compounds **24** and **26**) generally confer stronger receptor binding affinities than the *N*-methylpiperidine spirocycle (compound **31**).

However, the *N*-methylpiperidine in compound **31** appears to enhance anti-inflammatory properties despite reduced receptor binding, suggesting this structural element may influence signaling cascades beyond direct receptor interaction.

The cyclohexane spirocycle in compound **26** facilitates balanced receptor engagement while promoting Bcl-2 restoration and HIF-1 upregulation, indicating enhanced neuroprotective capabilities.

2'-Position substituent effects

Pyridin-3-yl substituent (**24**). Substantially enhances GABA(A) receptor binding, suggesting strong anxiolytic potential. Improves glutamate receptor binding, indicating possible cognitive enhancement properties. The nitrogen-containing aromatic ring likely forms additional hydrogen bonds within binding pockets.

Cyclohexyl substituent (**26**). Provides balanced binding across multiple targets, correlating with its comprehensive neuroprotective profile. The conformational flexibility of the cyclohexyl group may allow adaptable binding to diverse receptor architectures. This structural feature appears optimal for HIF-1 upregulation and Bcl-2 restoration, suggesting enhanced cell survival mechanism engagement.

Cyclopropyl substituent (**31**). Less favorable for direct receptor binding, particularly at dopamine and serotonin receptors. However, this structural feature appears to enhance anti-inflammatory and anti-inflammasome activity, suggesting specific interactions with inflammatory pathways. The compact, rigid cyclopropyl group may facilitate interactions with specific modulators of inflammatory cascades rather than neurotransmitter receptors.

2.7. Mechanistic Framework and Polypharmacology

The integration of molecular docking, neurobiochemical, and behavioral data suggests a complex mechanistic framework for these compounds:

Multi-target engagement hypothesis. The balanced binding profiles across multiple receptors, particularly for compounds **24** and **26**, align with contemporary understanding of effective cognitive enhancement requiring engagement of complementary pathways rather than strong interaction with a single receptor type, as highlighted by Jędrejko *et al.* [46].

Divergent primary mechanisms. Compound **26** appears to function primarily through enhanced cell survival pathways (Bcl-2 restoration) and adaptive responses (HIF-1 upregulation), facilitated by balanced receptor engagement. Compound **31** primarily modulates inflammatory pathways (IL-1β and caspase-1 reduction) with moderate receptor interaction, suggesting its mechanism involves

 doi:10.20944/preprints202504.0388.v1

signaling cascades downstream of receptor activation. Compound **24**'s strong GABA(A) and glutamate receptor binding suggests direct neurotransmitter system modulation as its primary mechanism.

*Structure-dependent signaling pathway activation***.** Cyclohexane spirocycle + cyclohexyl substituent (**26**): preferentially activates cell survival and hypoxic adaptation pathways. *N*-methylpiperidine spirocycle + cyclopropyl substituent (**31**): primarily modulates inflammatory signaling cascades. Cyclohexane spirocycle + pyridin-3-yl substituent (**24**): directly modulates inhibitory and excitatory neurotransmission.

2.8. Therapeutic Implications and Optimization Strategies

This integrated analysis provides rational guidance for therapeutic applications and further optimization:

Target-specific compound selection. For anti-anxiety applications with mild sedation: compound **24** (strongest GABA(A) binding). For neuroprotection with balanced cognitive effects: compound **26** (optimal Bcl-2 and HIF-1 modulation). For anti-neuroinflammatory applications with anxiolytic properties: compound **31** (superior anti-inflammatory profile)

Structural optimization approaches. For enhanced GABA(A) binding: incorporate pyridin-3-yl substituent at 2'-position. For balanced neuroprotection: utilize cyclohexyl substituent at 2'-position with cyclohexane spirocycle. For anti-inflammatory potency: explore modifications of the cyclopropyl-piperidine scaffold.

Hybrid compound development. Compounds incorporating features of both **26** and **31** might yield candidates with dual neuroprotective and anti-inflammatory properties. Hybrids of **24** and **26** could enhance both direct GABA(A) modulation and cell survival pathway activation.

2.9. Therapeutic Implications and Optimization Strategies

This integrated analysis suggests several promising research directions:

Receptor Binding Assays. Experimental validation of the computational docking predictions through radioligand binding studies to confirm target engagement.

Pathway-Specific Investigations. Examination of the effects of these compounds on specific signaling pathways, particularly inflammasome components, HIF-1 regulatory mechanisms, and Bcl-2 associated proteins.

Structure-Based Design. Utilization of the identified structure-activity relationships to design next-generation compounds with enhanced target selectivity or multi-target profiles.

Extended Behavioral Evaluation. Comprehensive behavioral assessment of compound **24** to validate its predicted anxiolytic potential based on exceptional GABA(A) binding.

Dose-Response Relationships. Investigation of dose-dependent effects on receptor binding, neurobiochemical markers, and behavioral outcomes to establish optimal therapeutic windows.

This integrated framework of molecular docking, neurobiochemical, and behavioral profiles provides a comprehensive understanding of these novel triazoloquinazoline derivatives, establishing a rational foundation for their further development as therapeutic agents for neuropsychiatric applications.

2.10. Limitations of The Study

There are several key limitations that should be acknowledged:

Methodological Limitations

Single-dose testing: The in *vivo* evaluation tested compounds at only one dose, limiting understanding of dose-response relationships and therapeutic windows. This prevents determination of optimal dosing regimens or potential toxicity at higher doses.

 doi:10.20944/preprints202504.0388.v1

Limited timeframe: The study appears to focus on acute effects following ketamine administration rather than long-term outcomes. The duration of neuroprotective effects and potential for sustained benefits remains unexplored.

Single animal model: Using only the ketamine-induced cognitive impairment model may limit generalizability to other types of cognitive disorders. Validation in additional models (e.g., traumatic brain injury, ischemia, or aging) would strengthen translational potential.

Sample size consideration: The study uses n=6-10 animals per group, which is relatively small. While likely sufficient to detect large effects, this sample size may limit detection of more subtle neuroprotective benefits or side effects.

Mechanistic Limitations

Indirect target validation: While molecular docking predicted binding to various receptors, direct receptor binding assays were not performed to confirm actual engagement with proposed targets.

Incomplete pathway analysis: The neurobiochemical investigation focused on selected markers (IL-1β, Bcl-2, caspase-1, MMP-9, c-fos, HIF-1) but did not comprehensively analyze all potential pathways involved in ketamine-induced neurotoxicity.

Limited pharmacokinetic data: The study lacks information on blood-brain barrier penetration, central nervous system exposure, or metabolic stability of the compounds, relying primarily on in silico predictions.

Translational Limitations

Sex differences unexplored: The study does not specify whether both male and female animals were used or address potential sex-based differences in drug responses, limiting generalizability.

Limited behavioral assessment: The behavioral evaluation relied primarily on the open field test. Additional cognitive assessment using tasks specifically focused on learning and memory (e.g., Morris water maze, novel object recognition) would strengthen the cognitive enhancement claims.

Species limitation: Using only rats limits extrapolation to human conditions without additional validation in other species or human cellular models.

Age considerations: The study used adult rats (6 months old) but did not explore how these compounds might affect developing or aging brains, which may have different sensitivities to ketamine neurotoxicity.

Technical Limitations

Structural characterization gaps: While spectral data were provided, X-ray crystallography confirmation of the three-dimensional structure was not included, which would be valuable for compounds where binding is predicted to depend on specific spatial arrangements.

Manufacturing considerations: The synthesis, while successful at laboratory scale, may face challenges in scale-up for potential clinical development.

3. Materials and Methods

3.1. Molecular Docking

CB-Dock2 [45,72], a protein-ligand auto blind docking tool, that inherits the curvature-based cavity detection procedure with AutoDock Vina, was used for calculations of tested substances' affinity to 10 macromolecules from RCSB Protein Data Bank, namely 5ZTY [34,73], 6HUP [71,74], 5ZKB [27,75], 6CM4 [36,76], 8FYX [35,77], (7XTC [30,78] 3LSX [43,79], 4K5Y [33,80], and 4OO9 [31,81] (Supplementary Materials, Table S1, S2, S6-S14). And the following substances were used as the references: JWH-133: (6*aR*,10*aR*)-6,6,9-trimethyl-3-(2-methylpentan-2-yl)-6*a*,7,10,10*a*-tetrahydrobenzo[*c*]chromene; diazepam: 7-chloro-1-methyl-5-phenyl-3*H*-1,4-benzodiazepin-2-one; AFDX-384: *N*-[2-[2-[(dipropylamino)methyl]piperidin-1-yl]ethyl]-6-oxo-5*H*-pyrido[2,3-*b*][1,4]benzodiazepine-11-carboxamide; etrumadenant: 3-[2-amino-6-[1-[[6-(2-hydroxypropan-2-yl)pyridin-2-yl]methyl]triazol-4-yl]pyrimidin-4-yl]-2-methylbenzonitrile; risperidone: 3-[2-[4-(6-fluoro-1,2-benzoxazol-3-yl)piperidin-1-yl]ethyl]-2-methyl-6,7,8,9-tetrahydropyrido[1,2-*a*]pyrimidin-

 doi:10.20944/preprints202504.0388.v1

4-one; buspirone: 8-[4-(4-pyrimidin-2-ylpiperazin-1-yl)butyl]-8-azaspiro[4.5]decane-7,9-dione; SB-269970: 3-[[(2*R*)-2-[2-(4-methyl-1-piperidinyl)ethyl]-1-pyrrolidinyl]sulfonyl]phenol; pramiracetam: *N*-[2-[di(propan-2-yl)amino]ethyl]-2-(2-oxopyrrolidin-1-yl)acetamide; CP-154,526: *N*-butyl-*N*-ethyl-2,5-dimethyl-7-(2,4,6-trimethylphenyl)-7*H*-pyrrolo[3,2-*e*]pyrimidin-4-amine; mavoglurant: methyl (3*aR*,4*S*,7*aR*)-4-hydroxy-4-[(3-methylphenyl)ethynyl]octahydro-1*H*-indole-1-carboxylate (Figure 1).

3.2. Synthesis

Melting points were measured in open capillary tubes using a «Mettler Toledo MP 50» apparatus (Columbus, USA). Elemental analyses (C, H, N) were conducted on an ELEMENTAR vario EL cube analyzer (Langenselbold, Germany), with the results for elements or functional groups deviating by no more than ± 0.3% from the theoretical values. The ^{1}H and ^{13}C NMR spectra (500 MHz) were obtained on a Varian Mercury 500 spectrometer (Varian Inc., Palo Alto, CA, USA), using TMS as an internal standard in a DMSO-*d6* solution. LC-MS data were acquired using a chromatography/mass spectrometric system comprising the high-performance liquid chromatography «Agilent 1100 Series» (Agilent, Palo Alto, CA, USA) equipped with a diode-matrix detector and mass-selective detector, «Agilent LC/MSD SL» (Agilent, Palo Alto, USA), with atmospheric pressure chemical ionization (APCI).

The starting substances **a** were obtained according to the previously described method and physicochemical constants that correspond to the literature data [41,82]. Synthetic studies (Figure 3) were carried out according to general approaches using reagents from «Merck» (Darmstadt, Germany), «Sigma-Aldrich» (Missouri, USA) and «Enamine» (Kyiv, Ukraine).

General procedure for the synthesis of 2′-R-6′*H*-spiro(cycloalkyl-, heterocyclyl)[1,2,4]triazolo[1,5-*c*]quinazolines (**1**-**40**):

To a solution of 10 mmol of the corresponding [2-(3-R-1*H*-1,2,4-triazolo-5-yl)phenyl]amine (**a**) in 10 ml of propanol-2 (or ethanol, propanol-1) was added 10 mmol of the corresponding ketone (cyclobutanone, cyclopentanone, cyclohexanone, 4-(*tert*-butyl)cyclohexan-1-one, 1-methyl-piperidone-4) and 2 drops of concentrated sulfate acid. The reaction mixture is left at room temperature for 24 hours (method A) or boiled for up to 6 hours (method B). Cool, pour into a 10% sodium acetate solution. The resulting precipitate is filtered and dried. Crystallize from methanol if necessary.

Synthesized compounds are white crystalline substances insoluble in water, soluble in alcohols, dioxane and DMF. Spectral data are found in the Supplementary Materials.

3.3. Toxicity Studies

A virtual lab of website ProTox-II was used for the prediction toxicities of molecules [51,83]. It incorporates molecular similarity, fragment propensities, most frequent features and (fragment similarity-based CLUSTER cross-validation) machine-learning, based a total of 33 models for the prediction of various toxicity endpoints such as acute toxicity, hepatotoxicity, cytotoxicity, carcinogenicity, mutagenicity, immunotoxicity, adverse outcomes (Tox21) pathways and toxicity targets. All methods, statistics of training set as well as the cross-validation results can be found at their website.

3.4. SwissADME Analysis

The SwissADME virtual laboratory was utilized to calculate the physicochemical descriptors and predict the ADME parameters, pharmacokinetic properties and drug-likeness [52,84]. The fundamental approaches and methodology underlying SwissADME, a free web-based tool designed for evaluating pharmacokinetics and drug-likeness, are detailed in the scientific literature.

 doi:10.20944/preprints202504.0388.v1

3.5. Biological Assay

3.5.1. Animals

The studies were performed on a sufficient number of animals, and all manipulations were carried out in accordance with the regulation on the use of animals in biomedical experiments (Council Directive 86/609/EEC) and the "General Ethical Principles of Animal Experiments" (EEC (1986). (Directive 2010/63/EU). The ZSMPhU Commission on Bioethics decided to adopt the experimental study protocols and outcomes (Protocol № 3, dated March 22, 2024). The design, execution, analysis, and reporting of the animal experiments in this study adhere to the Animal Research: Reporting of *In Vivo* Experiments (ARRIVE) guidelines.

The research was conducted on Wistar rats aged 6 months with a weight of 220-290 g, obtained from the breeding facility of the Institute of Pharmacology and Toxicology of the Academy of Medical Sciences of Ukraine. The quarantine (acclimatization) period for all animals was 14 days.

The animals were housed in polycarbonate cages measuring 550×320×180 mm with galvanized steel lids measuring 660×370×140 mm and glass drinking bottles. Each cage contained 5 rats. Every cage was labeled with information including the study number, species, sex, animal numbers, and dose. The cages were placed on shelves according to dosage levels and cage numbers indicated on the labels.

All rats were fed ad libitum a standard laboratory animal diet supplied by "Phoenix" company, Ukraine. Water from the municipal water supply (after reverse osmosis and UV sterilization) was provided without restriction. Alder (*Alnus glutinosa*) sawdust, previously treated by autoclaving, was used as bedding.

During the quarantine period, each animal was examined daily (behavior and general condition), and the animals were observed in their cages twice daily (for morbidity and mortality). Before starting the experiment, animals that met the inclusion criteria were randomly assigned to groups. Animals that did not meet the criteria were excluded from the experiment during quarantine.

The cages with animals were placed in separate rooms. Light regime: 12 hours light, 12 hours darkness. Air temperature was maintained within 19-25°C, and relative humidity at 50-70%. Temperature and humidity were recorded daily. Ventilation was set to provide approximately 15 room volumes per hour. The experimental animals were maintained on the same diet under standard vivarium conditions.

3.5.2. Behavioral Tests

Before conducting the experiment in the behavioral apparatus, the rats were randomly divided into nine groups: intact (**I**), control (**II**), and experimental (**III-IX**) groups, totaling n = 54 rats (n = 6 intact, 6 control, and 42 experimental rats).

The control (**II**) and experimental **(III** (piracetam), **IV** (fabomotizole), **V** (substance **33**), **VI** (**31**), **VII** (**32**), **VIII** (**25**), **IX** (**26**) groups received ketamine anesthesia through intraperitoneal administration of 100 mg/kg ketamine, in the form of an injection solution ("Ketamin," injection solution, 25 mg/ml, batch No. PC 04150085099096, manufacturer "Pfizer," Germany) [53–55].

After the animals recovered from ketamine anesthesia, the investigated compounds were administered to the experimental (**V-IX**) groups once at a dose of 10 mg/kg intraperitoneally as a suspension in Tween-80.

As reference drugs, the following ones were used. Piracetam was administered to rats in group **III** once at a dose of 250 mg/kg intraperitoneally as an injection solution ("Piracetam", injection solution in ampoules, 200 mg/ml, batch No. UA/0054/01/01, manufacturer UCB Pharma S.A., Belgium). Fabomotizole was administered to rats in group **IV** once at a dose of 10 mg/kg intraperitoneally as an extemporaneous aqueous solution ("Afobazole", 5-ethoxy-2-[2-(morpholino)ethyl]thio]benzimidazole, CAS:173352-21-1, manufacturer Sigma Aldrich, USA).

 doi:10.20944/preprints202504.0388.v1

The intact group (**I** group) received a single intraperitoneal dose of physiological saline at a rate of 1 ml per 100 g of weight. The control group (**II** group), after ketamine administration, also received a single intraperitoneal dose of physiological saline at the same dosage.

The determination of motor and exploratory activity was conducted using the "Open Field" method with a custom-made arena measuring 80×80×35 cm. Experiments were performed in a well-lit room in complete silence. During the experiments, the influence of external and internal visual, olfactory, and auditory stimuli was excluded.

The animal was placed near the middle of one side facing the wall, after which it was allowed to move freely around the arena for 8 minutes. We evaluated the following parameters:

- Total distance traveled (cm)
- Overall motor activity (cm^2/s)
- Activity structure (high activity, low activity, inactivity, %)
- Number of freezing episodes and entries into the center
- Distance traveled near the wall (cm) and in the central area of the arena (cm, %)
- Vertical exploratory activity (number of rearing on hind limbs near the wall and in the center)
- Number of short and long grooming events
- Number of defecation and urination acts

The assessment of animal behavior was conducted by a laboratory assistant who was unaware of the animal's specific experimental group assignment. Image capture and recording were performed using a SSC-DC378P color video camera (Sony, Japan). Video file analysis was conducted using Smartv 3.0 software (Harvard Apparatus, USA) [85].

Our behavioral assessment employed nuanced parameters in the "open field" test, analyzing total activity, high activity, and inactivity durations. This approach provides insights into the structural components of locomotor behavior that correlate with neurobiological changes. Total activity represents comprehensive movement patterns, while the computer-assisted analysis distinguishes between high activity and inactivity states. Activation pattern alterations in the amygdala - a limbic structure associated with fear and anxiety - differentiate between low and high activity states during "open field" testing, connecting behavioral outcomes to contextual fear conditioning. These behavioral manifestations correlate with c-fos expression levels in the amygdala and broader limbic system.

Elevated high activity percentage indicates reduced anxiety and fear responses, reflecting improved psycho-emotional status. Notably, significant increases in high activity and center entries can indicate pharmacological side effects, such as the agitated disorientation observed with amphetamine and certain antidepressants. Conversely, increased low activity and inactivity percentages directly correlate with depressive-like behaviors. Inactivity specifically associates with dopaminergic deficiency or reduced receptor affinity in the mesolimbic system. Activity structure alterations also reflect disruptions in serotonergic signaling, particularly in 5HT1A/5HT2A receptor ratios.

Fear and depression manifest behaviorally as thigmotaxis - extended time spent near the apparatus walls where lighting is diminished. The "freezing" parameter quantifies anxiety responses, while "free distance" and "center entries" demonstrate cognitive activity and absence of anxiety, fear, and depression.

3.5.3. Removal of Animals from the Experiment

Animal decapitation using ether anesthesia was performed on the 15th day after the termination of the experiment from 9:00 to 11:00.

At the end of the experiment, 3 hours after the administration of the last dose of the drug, the animals were decapitated using ether anesthesia and the brain was removed.

 doi:10.20944/preprints202504.0388.v1

3.5.4. Preparation of Biological Material

Blood was quickly removed from the brain, which was then separated from the meninges, and the studied pieces were placed in liquid nitrogen. Then they were crushed in liquid nitrogen to a powder-like state and homogenized in a 10-fold volume of medium at a temperature of (+2°C), which contained (in mmol): sucrose - 250 mM, tris-HCl buffer - 20 mM, EDTA - 1 mM (pH 7.4). At a temperature of (+4°C), the cytosolic and mitochondrial fractions were separated by differential centrifugation using a Sigma 3-30k refrigerated centrifuge (Germany). To purify the fraction from large cellular fragments, preliminary centrifugation was performed for 7 minutes at 1000g, and then the supernatant was re-centrifuged for 20 minutes at 17000g. The supernatant was decanted and stored at -80°C. A portion of the brain was placed in Bouin's fixative for 24 hours. After the standard procedure of tissue dehydration and its impregnation with chloroform and paraffin, the brain pieces were embedded in paraplast (MkCormick, USA). Serial histological sections of the CA-1 zone of the hippocampus with a thickness of 5 μm were prepared on a Microm-325 rotational microscope (Microm Corp., Germany), which after processing with o-xylol and ethanol were used for real-time PCR research.

3.5.5. Polymerase Chain Reaction in Real Time

To determine the expression level of c-fos mRNA and HIF-1S mRNA, a CFX96 RT-PCR Detection Systems amplifier (Bio-Rad Laboratories, Inc., USA) was used. In our studies, for PCR under time conditions, there were a set of reagents manufactured by Sintol, russia (No. R-415) that were used. The amplification composition included SYBR Green dye, SynTaq DNA polymerase with antibodies inhibiting enzyme activity, 0.2 μl each of forward and reverse-specific primers, dNTP-deoxynucleoside triphosphates, and 1 μl of matrix (cDNA). The reaction mixture was adjusted to a total volume of 25 μl by adding deionized water. Specific primer pairs (5′-3′) for analysis of the studied and reference genes were selected using the PrimerBlast software (www.ncbi.nlm.nih.gov/tools/primer-blast) and manufactured by ThermoScientific, USA. Amplification took place under the following conditions: initiated denaturation 95°C – 10 min; further, 50 cycles: denaturation – 95°C, 15 s., primer annealing – 58–63°C, 30 s., and elongation – 72°C, 30 s. Registration of fluorescence intensity occurred automatically at the end of the elongation stage of each cycle through the automatic SybrGreen channel. The actin and beta (Actb) gene were used as a reference gene to determine the relative value of changes in the expression level of the studied genes.

3.5.7. Statistical Analysis

Experimental data were statistically analyzed using “StatisticaR for Windows 6.0” (StatSoft Inc., Tulsa, OK, USA, AXXR712D833214FAN5), “SPSS16.0”, and “Microsoft Office Excel 2010” software. Prior to statistical tests, we checked the results for normality (Shapiro–Wilk and Kolmogorov–Smirnov tests). In the normal distribution, intergroup differences were considered statistically significant based on the parametric Student’s t-test. If the distribution was not normal, the comparative analysis was conducted using the non-parametric Mann–Whitney U-test. To compare independent variables in more than two selections, we applied ANOVA dispersion analysis for the normal distribution and the Kruskal–Wallis test for the non-normal distribution. To analyze correlations between parameters, we used correlation analysis based on the Pearson or Spearman correlation coefficient. For all types of analysis, the differences were considered statistically significant at $p < 0.05$ (95%).

4. Conclusions

This study comprehensively examines the development of novel 2'-R-6'*H*-spiro(cycloalkyl-, heterocyclyl)[1,2,4]triazolo[1,5-*c*]quinazolines as potential neuroprotective agents for cognitive and behavioral disorders following ketamine anesthesia. Through integrated computational, synthetic,

 doi:10.20944/preprints202504.0388.v1

and biological approaches, we have identified several promising compounds with superior profiles compared to established reference drugs.

The rational design strategy, incorporating key structural features from clinically validated pharmacophores, yielded a focused library of compounds with optimized drug-like properties. Molecular docking studies revealed that most compounds demonstrated significant affinity for multiple targets involved in neuroprotection and cognition, particularly with the glutamate receptor GluA3, with binding energies exceeding those of reference compounds piracetam and pramiracetam.

In silico ADMET evaluations indicated favorable toxicity profiles and drug-likeness parameters for the selected compounds, with most derivatives meeting established criteria for bioavailability and blood-brain barrier permeation. In *vivo* behavioral studies using the ketamine-induced cognitive impairment model revealed that compounds **25**, **26**, and **32** demonstrated superior efficacy in normalizing behavioral parameters, reducing anxiety-like behaviors, and improving cognitive function compared to piracetam and fabomotizole. Notably, compounds **31** and **26** exhibited distinct neurobiochemical profiles, with compound 31 showing superior anti-inflammatory properties and compound **26** demonstrating enhanced effects on cell survival pathways.

Detailed structure-activity relationship analyses established that, the spiro-junction significantly influences pharmacological activity, with cyclohexane spirocycles (**25**, **26**) promoting normalized behavior and *N*-methylpiperidine derivatives (**31**-**33**) exhibiting diverse profiles depending on the 2'-substituent. The 2'-position substituent critically determines the behavioral and molecular effects, with cyclohexyl substitution (**26**, **32**) normalizing hyperactivity and cyclopropyl-*N*-methylpiperidine (**31**) demonstrating anxiolytic and anti-inflammatory properties. Molecular docking revealed specific binding interactions that correlate with observed behavioral effects, particularly for GABA(A) and M2 muscarinic receptors.

The pronounced efficacy of these compounds in attenuating neuroinflammation, reducing caspase-1-mediated pyroptosis, restoring anti-apoptotic Bcl-2 levels, and upregulating HIF-1 expression suggests multifaceted neuroprotective mechanisms that address the complex pathophysiology of ketamine-induced neurotoxicity.

This work establishes 2'-R-6'*H*-spiro(cycloalkyl-, heterocyclyl)[1,2,4]triazolo[1,5-*c*]quinazolines as a promising structural class for developing neuroprotective agents with potential applications extending beyond ketamine-induced cognitive dysfunction to post-COVID neurological sequelae and trauma-related neuropsychiatric conditions. Future research should focus on optimizing lead compounds through targeted structural modifications, elucidating precise molecular mechanisms through receptor binding studies, and evaluating efficacy in diverse neurological disorder models.

These findings not only advance our understanding of structure-activity relationships in triazoloquinazoline-based neuroprotectants but also provide rational frameworks for developing multi-target therapeutic strategies for complex neurological conditions characterized by cognitive dysfunction, anxiety, and neuroinflammation.

Supplementary Materials: The following supporting information can be downloaded at the website of this paper posted on Preprints.org, Spectral data of compounds **1**-**40**. **Table S1.** Effect of the studied compounds on animal behavior indicators in the open field after ketamine anesthesia; **Table S2.** Effect of the studied compounds on the concentration of molecular markers in the cytosolic fraction of rat brain after ketamine anesthesia; **Table S3.** Effect of the studied compounds on the expression of c-fos mRNA and HIF-1 mRNA in the CA1 zone of the rat brain hippocampus after ketamine anesthesia; **Table S4**. Binding affinities, calculated in the pocket for reference substances *via* CB-Dock2 website, towards nootropic and anxiolytic targets downloaded from RCSB Protein Data Bank (kcal/mol); **Table S5.** Comparative binding affinities of compounds to nootropic and anxiolytic receptor targets: alternative binding pocket analysis *via* CB-Dock2 (kcal/mol); **Table S6.** Calculated affinity of compounds towards glutamate receptor 3 (GluA3) (PDB ID: 3LSX); **Table S7**. Calculated affinity of compounds towards full-length alpha1/beta3/gamma2L GABAA (PDB ID: 6HUP); **Table S8.** Calculated affinity of compounds towards G protein coupled receptor (PDB ID: 5ZTY); **Table S9.** Calculated affinity of compounds towards M2 muscarinic acetylcholine receptor (PDB ID: 5ZKB); **Table S10**. Calculated

 doi:10.20944/preprints202504.0388.v1

affinity of compounds towards D2 dopamine receptor (PDB ID: 6CM4); **Table S11.** Calculated affinity of compounds towards serotonin 1A (5-HT1A) receptor-Gi1 protein (PDB ID: 8FYX); **Table S12**. Calculated affinity of compounds towards serotonin 7 (5-HT7) receptor-Gs-Nb35 (PDB ID: 7XTC); **Table S13**. Calculated affinity of compounds towards corticotropin-releasing factor receptor 1 (CRF1R) (PDB ID: 4K5Y); **Table S14.** Calculated affinity of compounds towards human class C GPCR metabotropic glutamate receptor 5 transmembrane domain (PDB ID: 4OO9). ^{1}H NMR, ^{13}C NMR and LC-MS spectra of compounds.

Author Contributions: K.S., L.A., I.B., S.K.: Conceptualization, Methodology, Investigation, Formal Analysis, Software, Writing—Original Draft, Visualization, Writing—Review and Editing; N.B., V.R.: Investigation, Data curation; I.B., S.K., V.O., O.K.: Validation, Resources, Project administration, Supervision; S.K.: Funding Acquisition. All authors have read and agreed to the published version of the manuscript.

Funding: This work was funded by the Ministry of Education and Science of Ukraine, № 0125U001851, the name of the project "New azaheterocycles: molecular design, synthesis, prospects for use for pharmacocorrection of post-traumatic stressful disorders and metabolic syndrome".

Institutional Review Board Statement: The studies were performed on a sufficient number of animals, and all manipulations were carried out in accordance with the regulation on the use of animals in biomedical experiments (Council Directive 86/609/EEC) and the "General Ethical Principles of Animal Experiments" (EEC (1986). (Directive 2010/63/EU). The ZSMPhU Commission on Bioethics decided to adopt the experimental study protocols and outcomes (Protocol № 3, dated March 22, 2024).

Data Availability Statement: The data presented in this study are available on request from the corresponding author. The Supplementary Materials are available free of charge on the MDPI Publication website.

Acknowledgments: Authors gratefully acknowledge Armed Forces of Ukraine with Territorial Defense Forces of the Armed Forces of Ukraine for preparing this paper in the safe conditions of Zaporizhzhia, Ukraine; and assistance of large language model Claude 3.7 by Anthropic during manuscript preparation in English language.

Conflicts of Interest: The authors declare no conflicts of interest.

Abbreviations

The following abbreviations are used in this manuscript:

POCD	Postoperative Cognitive Dysfunction
CNS	Central Nervous System
HIF-1	Hypoxia-Inducible Factor 1
IL-1β	Interleukin-1 Beta
AMPA	α-Amino-3-Hydroxy-5-Methyl-4-Isoxazole Propionic Acid
GABA	Gamma-Aminobutyric Acid
5-HT	5-Hydroxytryptamine (Serotonin)
mGluR5	Metabotropic Glutamate Receptor 5
CRF1R	Corticotropin-Releasing Factor Receptor 1
CB_2	Cannabinoid Receptor Type 2
NMDA	N-Methyl-D-Aspartate
ROS	Reactive Oxygen Species
i-NOS	Inducible Nitric Oxide Synthase
n-NOS	Neuronal Nitric Oxide Synthase
SAR	Structure-Activity Relationship
MW	Molecular Weight

 doi:10.20944/preprints202504.0388.v1

n-ROTB	Number of Rotatable Bonds
n-HBA	Number of Hydrogen Bond Acceptors
n-HBD	Number of Hydrogen Bond Donors
TPSA	Topological Polar Surface Area
logP	Octanol-Water Partition Coefficient
MMP-9	Matrix Metalloproteinase-9
Bcl-2	B-cell Lymphoma 2
ADMET	Absorption, Distribution, Metabolism, Excretion, and Toxicity
GluA3	Glutamate Receptor AMPA Type Subunit 3
PCR	Polymerase Chain Reaction
ELISA	Enzyme-Linked Immunosorbent Assay
M2	Muscarinic Acetylcholine Receptor M2
D2	Dopamine Receptor D2

References

1. Leslie, E.; Pittman, E.; Drew, B.; Walrath, B. Ketamine Use in Operation Enduring Freedom. *Mil. Med.* **2021**, *186*, e720–e725. https://doi.org/10.1093/milmed/usab117
2. Butler, F.K. Tactical Combat Casualty Care: Beginnings. *Wilderness Environ. Med.* **2017**, *28*, S12–S17. https://doi.org/10.1016/j.wem.2016.12.004
3. Barr, J.; Fraser, G.L.; Puntillo, K.; Ely, E.W.; Gélinas, C.; Dasta, J.F.; Davidson, J.E.; Devlin, J.W.; Kress, J.P.; Joffe, A.M.; et al. Clinical practice guidelines for the management of pain, agitation, and delirium in adult patients in the intensive care unit. *Crit. Care Med.* **2013**, *41*, 263–306. https://doi.org/10.1097/CCM.0b013e3182783b72
4. Cohen, B.; Talmy, T.; Gelikas, S.; Radomislensky, I.; Kontorovich-Chen, D.; Cohen, B.; Bar-Or, D.; Almog, O.; Glassberg, E. Opioid sparing effect of ketamine in military prehospital pain management-A retrospective study. *J. Trauma Acute Care Surg.* **2022**, *93*, S71–S77. https://doi.org/10.1097/TA.0000000000003695
5. Riccardi, A.; Guarino, M.; Serra, S.; Spampinato, M.D.; Vanni, S.; Shiffer, D.; Voza, A.; Fabbri, A.; De Iaco, F. Low-Dose Ketamine for Pain Management. *J. Clin. Med.* **2023**, *12*, 3256. https://doi.org/10.3390/jcm12093256.
6. Li, L.; Vlisides, P.E. Ketamine: 50 Years of Modulating the Mind. *Front. Hum. Neurosci.* **2016**, *10*, 612. https://doi.org/10.3389/fnhum.2016.00612
7. Hashimoto, K. Detrimental Side Effects of Repeated Ketamine Infusions in the Brain. *Am. J. Psychiatry* **2016**, *173*, 1044–1045. https://doi.org/10.1176/appi.ajp.2016.16040411
8. Pereira, H.; Antunes, M.V.; Teles, D.; Pereira, L.G.; Abelha, F. Association between intraoperative ketamine and the incidence of emergence delirium in laparoscopic surgeries: an observational study. *Braz. J. Anesthesiol.* **2024**, *74*, 744414. https://doi.org/10.1016/j.bjane.2022.10.002
9. Viderman, D.; Aubakirova, M.; Nabidollayeva, F.; Yegembayeva, N.; Bilotta, F.; Badenes, R.; Thorat, A.A.; Yeseuleukova, S.; Baynazar, D.; Yerkinova, A.; et al. Effect of Ketamine on Postoperative Neurocognitive Disorders: A Systematic Review and Meta-Analysis. *J. Clin. Med.* **2023**, *12*, 4314. https://doi.org/10.3390/jcm12134314
10. Belenichev, I.; Burlaka, B.; Puzyrenko, A.; Ryzhenko, O.; Kurochkin, M.; Yusuf, J. Management of amnestic and behavioral disorders after ketamine anesthesia. *Georgian Med. News* **2019**, *294*, 141–145.
11. Chen, M.; Han, Y.; Que, B.; Zhou, R.; Gan, J.; Dong, X. Prophylactic Effects of Sub-anesthesia Ketamine on Cognitive Decline, Neuroinflammation, and Oxidative Stress in Elderly Mice. *Am. J. Alzheimers Dis. Other Demen.* **2022**, *37*. https://doi.org/10.1177/15333175221141531
12. Ma, J.; Wang, F.; Wang, J.; Wang, P.; Dou, X.; Yao, S.; Dong, X.; Luo, J. The Effect of Low-Dose Esketamine on Postoperative Neurocognitive Dysfunction in Elderly Patients Undergoing General Anesthesia for

 doi:10.20944/preprints202504.0388.v1

Gastrointestinal Tumors: A Randomized Controlled Trial. *Drug Des. Devel. Ther.* **2023**, *17*, 1945–1957. https://doi.org/10.2147/DDDT.S406568

13. Lee, K.H.; Kim, J.Y.; Kim, J.W.; Park, J.S.; Lee, K.W.; Jeon, S.Y. Influence of Ketamine on Early Postoperative Cognitive Function After Orthopedic Surgery in Elderly Patients. *Anesth. Pain Med.* **2015**, *5*, e28844. https://doi.org/10.5812/aapm.28844
14. Haller, G.; Chan, M.T.V.; Combescure, C.; Lopez, U.; Pichon, I.; Licker, M.; Baele, P.; Bailie, R.; de Haever, G.; Ellerkmann, R.; et al. The international ENIGMA-II substudy on postoperative cognitive disorders (ISEP). *Sci. Rep.* **2021**, *11*, 11631. https://doi.org/10.1038/s41598-021-91014-8
15. Fang, Y.; Qiu, Z.; Hu, W.; Yang, J.; Yi, X.; Huang, L.; Zhang, S. Effect of piracetam on the cognitive performance of patients undergoing coronary bypass surgery: A meta-analysis. *Exp. Ther. Med.* **2014**, *7*, 429–434. https://doi.org/10.3892/etm.2013.1425
16. Belenichev, I.F.; Burlaka, B.S.; Ryzhenko, O.I.; Ryzhenko, V.P.; Aliyeva, O.G.; Makyeyeva, L.V. Neuroprotective and anti-apoptotic activity of the IL-1 antagonist RAIL-gel in rats after ketamine anesthesia. *Pharmakeftiki* **2021**, *33*, 97–106.
17. Belenichev, I.; Popazova, O.; Bukhtiyarova, N.; Savchenko, D.; Oksenych, V.; Kamyshnyi, O. Modulating Nitric Oxide: Implications for Cytotoxicity and Cytoprotection. *Antioxidants* **2024**, *13*, 504. https://doi.org/10.3390/antiox13050504
18. Usenko, L.; Krishtafor, A.; Polinchuk, I.; Tiutiunnik, A.; Usenko, A.; Petrashenok, Y. Postoperative Cognitive Dysfunction as a Complication of General Anesthesia. The Importance of Early Pharmacological Neuroprotection. *EMERGENCY MEDICINE* **2015**, *2*, 24–31. https://doi.org/10.22141/2224-0586.2.65.2015.79419
19. Colucci, L.; Bosco, M.; Rosario Ziello, A.; Rea, R.; Amenta, F.; Fasanaro, A.M. Effectiveness of nootropic drugs with cholinergic activity in treatment of cognitive deficit: a review. *J. Exp. Pharmacol.* **2012**, *4*, 163–172. https://doi.org/10.2147/JEP.S35326
20. Dirks, B.; Seibert, A.; Sperling, G.; Krieglstein, J. Vergleich der Wirkungen von Piracetam und Methohexital auf den zerebralen Energiestoffwechsel [Comparison of the effects of piracetam and methohexital on cerebral energy metabolism]. *Arzneimittelforschung* **1984**, *34*, 258–266.
21. Belenichev, I.; Gorchakova, N.; Kuchkovskyi, O.; Ryzhenko, V.; Varavka, I.; Varvanskyi, P.; Levchenko, K.; Yusuf, J. Principles of metabolithotropic therapy in pediatric practice. Clinical and pharmacological characteristics of modern metabolithotropic agents (part 2). *Phytother. J.* **2022**, *4*, 5–29. https://doi.org/10.33617/2522-9680-2022-4-5
22. Belenichev, I.; Popazova, O.; Bukhtiyarova, N.; Ryzhenko, V.; Pavlov, S.; Suprun, E.; Tykhomyrov, A.; Zadoya, A.; Kaplaushenko, A.; Belenichev, I.; et al. Targeting Mitochondrial Dysfunction in Cerebral Ischemia: Advances in Pharmacological Interventions. *Antioxidants* **2025**, *14*, 108. https://doi.org/10.3390/antiox14010108
23. Sarawagi, A.; Soni, N.D.; Patel, A.B. Glutamate and GABA Homeostasis and Neurometabolism in Major Depressive Disorder. *Front. Psychiatry* **2021**, *12*, 637863. https://doi.org/10.3389/fpsyt.2021.637863
24. Aznar, S.; Hervig, M.-S. The 5-HT2A serotonin receptor in executive function: Implications for neuropsychiatric and neurodegenerative diseases. *Neurosci. Biobehav. Rev.* **2016**, *64*, 63–82. https://doi.org/10.1016/j.neubiorev.2016.02.008
25. Sheng, J.A.; Bales, N.J.; Myers, S.A.; Bautista, A.I.; Roueinfar, M.; Hale, T.M.; Handa, R.J. The Hypothalamic-Pituitary-Adrenal Axis: Development, Programming Actions of Hormones, and Maternal-Fetal Interactions. *Front. Behav. Neurosci.* **2021**, *14*, 601939. https://doi.org/10.3389/fnbeh.2020.601939
26. Smith, C.; Gentleman, S.M.; Leclercq, P.D.; Murray, L.S.; Griffin, W.S.; Graham, D.I.; Nicoll, J.A. The neuroinflammatory response in humans after traumatic brain injury. *Neuropathol. Appl. Neurobiol.* **2013**, *39*, 654–666. https://doi.org/10.1111/nan.12008
27. Suno, R.; Lee, S.; Maeda, S.; Yasuda, S.; Yamashita, K.; Hirata, K.; Horita, S.; Tawaramoto, M.S.; Tsujimoto, H.; Murata, T.; et al. Structural insights into the subtype-selective antagonist binding to the M2 muscarinic receptor. *Nat. Chem. Biol.* **2018**, *14*, 1150–1158. https://doi.org/10.1038/s41589-018-0152-y
28. Winblad, B. Piracetam: A Review of Pharmacological Properties and Clinical Uses. *CNS Drug Rev.* **2005**, *11*, 169–182. https://doi.org/10.1111/j.1527-3458.2005.tb00268.x

 doi:10.20944/preprints202504.0388.v1

29. Gouhie, F.A.; Barbosa, K.O.; Cruz, A.B.R.; Wellichan, M.M.; Zampolli, T.M. Cognitive effects of piracetam in adults with memory impairment: A systematic review and meta-analysis. *Clin. Neurol. Neurosurg.* **2024**, *243*, 108358. https://doi.org/10.1016/j.clineuro.2024.108358
30. Hagan, J.J.; Price, G.W.; Jeffrey, P.; Deeks, N.J.; Stean, T.; Piper, D.; Smith, M.I.; Upton, N.; Medhurst, A.D.; Middlemiss, D.N.; et al. Characterization of SB-269970-A, a selective 5-HT(7) receptor antagonist. *Br. J. Pharmacol.* **2000**, *130*, 539–548. https://doi.org/10.1038/sj.bjp.0703357
31. Doré, A.S.; Okrasa, K.; Patel, J.C.; Serrano-Vega, M.; Bennett, K.; Cooke, R.M.; Errey, J.C.; Jazayeri, A.; Khan, S.; Tehan, B.; et al. Structure of class C GPCR metabotropic glutamate receptor 5 transmembrane domain. *Nature* **2014**, *511*, 557–562. https://doi.org/10.1038/nature13396
32. MedKoo Biosciences [Internet]. fabomotizole dihydrochloride | CAS# 189638-30-0 (2HCl) | Anxiolytic | MedKoo; [cited 2025 Mar 17]. Available online: https://www.medkoo.com/products/32719 (accessed on 17 March 2025).
33. Seymour, P.A.; Schmidt, A.W.; Schulz, D.W. The pharmacology of CP-154,526, a non-peptide antagonist of the CRH1 receptor: a review. *CNS Drug Rev.* **2003**, *9*, 57–96. https://doi.org/10.1111/j.1527-3458.2003.tb00244.x
34. Ivy, D.; Palese, F.; Vozella, V.; Fotio, Y.; Yalcin, A.; Ramirez, G.; Mears, D.; Winder, D.G.; Cristino, L.; Piomelli, D.; et al. Cannabinoid CB2 receptors mediate the anxiolytic-like effects of monoacylglycerol lipase inhibition in a rat model of predator-induced fear. *Neuropsychopharmacology* **2020**, *45*, 1330–1338. https://doi.org/10.1038/s41386-020-0696-x
35. Li, Q.; Luo, T.; Jiang, X.; Wang, J. Anxiolytic effects of 5-HT_1A receptors and anxiogenic effects of 5-HT_2C receptors in the amygdala of mice. *Neuropharmacology* **2012**, *62*, 474–484. https://doi.org/10.1016/j.neuropharm.2011.09.002
36. Wang, S.; Che, T.; Levit, A.; Shoichet, B.K.; Wacker, D.; Roth, B.L. Structure of the D2 dopamine receptor bound to the atypical antipsychotic drug risperidone. *Nature* **2018**, *555*, 269–273. https://doi.org/10.1038/nature25758
37. Zheng, Y.; Tice, C.M.; Singh, S.B. The use of spirocyclic scaffolds in drug discovery. *Bioorg. Med. Chem. Lett.* **2014**, *24*, 3673–3682. https://doi.org/10.1016/j.bmcl.2014.06.081
38. Batista, V.F.; Pinto, D.C.G.A.; Silva, A.M.S. Recent in vivo advances of spirocyclic scaffolds for drug discovery. *Expert Opin. Drug Discov.* **2022**, *17*, 603–618. https://doi.org/10.1080/17460441.2022.2055544
39. Basavaraja, D.; Doddamani, S.V.; Athira, C.S.; Siby, A.; Sreelakshmi, V.; Ancy, A.; Azeez, S.; Babu, T.S.; Manjula, S.N.; Rangappa, K.S.; et al. Spiro-heterocycles: Recent advances in biological applications and synthetic strategies. *Tetrahedron* **2025**, *173*, 134468. https://doi.org/10.1016/j.tet.2025.134468
40. Kolomoets, O.; Voskoboynik, O.; Antypenko, O.; Berest, G.; Nosulenko, I.; Palchikov, V.; Karpenko, O.; Andronati, S.; Kovalenko, S. Design, synthesis and anti-inflammatory activity of derivatives 10-R-3-aryl-6,7-dihydro-2H-[1,2,4]triazino[2,3-c]quinazolin-2-ones of spiro-fused cyclic frameworks. *Acta Chim. Slov.* **2017**, *64*, 902–910. https://doi.org/10.17344/acsi.2017.3575
41. Kholodnyak, S.V.; Schabelnyk, K.P.; Antypenko, O.M.; Kovalenko, S.I.; Palchykov, V.A.; Okovyty, S.I.; Shishkina, S.V. 5,6-Dihydro-[1,2,4]triazolo[1,5-c]quinazolines. Message 4. Spirocompounds with [1,2,4]triazolo[1,5-c]quinazolines moieties. Synthesis and spectral characteristics. *J. Org. Pharm. Chem.* **2016**, *14*, 24–31. https://doi.org/10.24959/ophcj.16.897
42. Kholodnyak, S.V.; Bukhtiarova, N.V.; Shabelnyk, K.P.; Berest, G.G.; Belenichev, I.F.; Kovalenko, S.I. Targeted search for anticonvulsant agents among spiroderivatives with 2-aryl-5,6-dihydro[1,2,4]triazolo[1,5-c]quinazoline fragment. *Pharmacol. Drug Toxicol.* **2016**, *1(47)*, 39–47.
43. Ahmed, A.H.; Oswald, R.E. Piracetam defines a new binding site for allosteric modulators of α-amino-3-hydroxy-5-methyl-4-isoxazole-propionic acid (AMPA) receptors. *J. Med. Chem.* **2010**, *53*, 2197–2203. https://doi.org/10.1021/jm901905j
44. Tanimukai, H.; Kudo, T.; Tanaka, T.; Grundke-Iqbal, I.; Iqbal, K.; Takeda, M. Novel therapeutic strategies for neurodegenerative disease. *Psychogeriatrics* **2009**, *9*, 103–109. https://doi.org/10.1111/j.1479-8301.2009.00289.x

 doi:10.20944/preprints202504.0388.v1

45. Liu, Y.; Yang, X.; Gan, J.; Chen, S.; Xiao, Z.X.; Cao, Y. CB-Dock2: Improved Protein-Ligand Blind Docking by Integrating Cavity Detection, Docking and Homologous Template Fitting. *Nucleic Acids Res.* **2022**, *50*, W159–W164. https://doi.org/10.1093/nar/gkac394
46. Jędrejko, K.; Catlin, O.; Stewart, T.; Anderson, A.; Muszyńska, B.; Catlin, D.H. Unauthorized ingredients in "nootropic" dietary supplements: A review of the history, pharmacology, prevalence, international regulations, and potential as doping agents. *Drug Test. Anal.* **2023**, *15*, 803–839. https://doi.org/10.1002/dta.3529
47. Antypenko, L.; Shabelnyk, K.; Antypenko, O. Anxiolytic potential of 1-methyl/4-(*tert*-butyl)-2'-(cycloalkyl/hetaryl)-6'*H*-spiro[piperidine/cycloalkane-4,5'/1,5'-[1,2,4]triazolo[1,5-*c*]quinazolines]. In *Proceedings of the VII International Scientific and Theoretical Conference "Scientific forum: theory and practice of research"*, Valencia, Spain, 31 January 2025; pp. 307–310. https://doi.org/10.36074/scientia-31.01.2025
48. Pylypenko, O.O.; Sviatenko, L.K.; Shabelnyk, K.P.; Kovalenko, S.I.; Okovytyy, S.I. Reaction of [2-(3-hetaryl-1,2,4-triazol-5-yl)phenyl]amines with ketones. DFT study. *Theor. Chem. Acc.* **2024**, *143*, 35. https://doi.org/10.1007/s00214-024-03110-3
49. Breitmaier, E. Structure Elucidation by NMR in Organic Chemistry: A Practical Guide, 3rd ed.; Wiley: Chichester, UK, 2002.
50. Antypenko, L.; Shabelnyk, K.; Antypenko, O.; Kovalenko, S.; Arisawa M. *In silico* identification and characterization of spiro[1,2,4]triazolo[1,5-*c*]quinazolines as next-generation diacylglycerol kinase α modulators. **2025**, under submission.
51. Banerjee, P.; Kemmler, E.; Dunkel, M.; Preissner, R. ProTox 3.0: a webserver for the prediction of toxicity of chemicals. *Nucleic Acids Res.* **2024**, *52*, W513–W520. https://doi.org/10.1093/nar/gkae303
52. Daina, A.; Michielin, O.; Zoete, V. SwissADME: a free web tool to evaluate pharmacokinetics, drug-likeness and medicinal chemistry friendliness of small molecules. *Sci. Rep.* **2017**, *7*. https://doi.org/10.1038/srep42717
53. Duman, R.S.; Li, N.; Liu, R.J.; Duric, V.; Aghajanian, G. Signaling pathways underlying the rapid antidepressant actions of ketamine. *Neuropharmacology* **2012**, *62*, 35–41. https://doi.org/10.1016/j.neuropharm.2011.08.044
54. Zanos, P.; Gould, T.D. Mechanisms of ketamine action as an antidepressant. *Mol. Psychiatry* **2018**, *23*, 801–811. https://doi.org/10.1038/mp.2017.255
55. Krystal, J.H.; Abdallah, C.G.; Sanacora, G.; Charney, D.S.; Duman, R.S. Ketamine: A Paradigm Shift for Depression Research and Treatment. *Neuron* **2019**, *101*, 774–778. https://doi.org/10.1016/j.neuron.2019.02.005
56. Xia, Z.; Dudek, H.; Miranti, C.K.; Greenberg, M.E. Calcium influx via the NMDA receptor induces immediate early gene transcription by a MAP kinase/ERK-dependent mechanism. *J. Neurosci.* **1996**, *16*, 5425–5436. https://doi.org/10.1523/JNEUROSCI.16-17-05425.1996
57. Simões, A.P.; Silva, C.G.; Marques, J.M.; Pochmann, D.; Porciúncula, L.O.; Ferreira, S.; Carvalho, A.R.; Canas, P.M.; Andrade, G.M.; Fontes-Ribeiro, C.A.; et al. Glutamate-induced and NMDA receptor-mediated neurodegeneration entails P2Y1 receptor activation. *Cell Death Dis.* **2018**, *9*, 297. https://doi.org/10.1038/s41419-018-0351-1
58. Behrooz, A.B.; Nasiri, M.; Adeli, S.; Jafarian, M.; Pestehei, S.K.; Babaei, J.F. Pre-adolescence repeat exposure to sub-anesthetic doses of ketamine induces long-lasting behaviors and cognition impairment in male and female rat adults. *IBRO Neurosci. Rep.* **2024**, *16*, 211–223. https://doi.org/10.1016/j.ibneur.2024.01.005
59. Lei, X.; Guo, Q.; Zhang, J. Mechanistic Insights into Neurotoxicity Induced by Anesthetics in the Developing Brain. *Int. J. Mol. Sci.* **2012**, *13*, 6772–6799. https://doi.org/10.3390/ijms13066772
60. Zhang, D.; Liu, J.; Zhu, T.; Zhou, C. Identifying c-fos Expression as a Strategy to Investigate the Actions of General Anesthetics on the Central Nervous System. *Curr. Neuropharmacol.* **2022**, *20*, 55–71. https://doi.org/10.2174/1570159X19666210909150200
61. Massara D., L.; Osuru, H.P.; Oklopcic, A.; Milanovic, D.; Joksimovic, S.M.; Caputo, V.; DiGruccio, M.R.; Ori, C.; Wang, G.; Todorovic, S.M.; et al. General Anesthesia Causes Epigenetic Histone Modulation of c-Fos and Brain-derived Neurotrophic Factor, Target Genes Important for Neuronal Development in the Immature Rat Hippocampus. *Anesthesiology* **2016**, *124*, 1311–1327. https://doi.org/10.1097/ALN.0000000000001111

 doi:10.20944/preprints202504.0388.v1

62. Fidalgo, A.R.; Cibelli, M.; White, J.P.; Nagy, I.; Maze, M.; Ma, D. Systemic inflammation enhances surgery-induced cognitive dysfunction in mice. *Neurosci. Lett.* **2011**, *498*, 63–66. https://doi.org/10.1016/j.neulet.2011.04.063
63. Ye, Z.; Li, Q.; Guo, Q.; Xiong, Y.; Guo, D.; Yang, H.; Yang, L. Ketamine induces hippocampal apoptosis through a mechanism associated with the caspase-1 dependent pyroptosis. *Neuropharmacology* **2018**, *128*, 63–75. https://doi.org/10.1016/j.neuropharm.2017.09.035
64. Wu, L.; Zhang, K.; Sun, L.; Bai, J.; Zhang, M.; Zheng, J. Laminin degradation by matrix metalloproteinase 9 promotes ketamine-induced neuronal apoptosis in the early developing rat retina. *CNS Neurosci. Ther.* **2020**, *26*, 1058–1068. https://doi.org/10.1111/cns.13428
65. Belenichev, I.F.; Aliyeva, O.G.; Popazova, O.O.; Bukhtiyarova, N.V. Involvement of heat shock proteins HSP70 in the mechanisms of endogenous neuroprotection: the prospect of using HSP70 modulators. *Front. Cell Neurosci.* **2023**, *17*, 1131683. https://doi.org/10.3389/fncel.2023.1131683
66. Farahmandfar, M.; Akbarabadi, A.; Bakhtazad, A.; Zarrindast, M.R. Recovery from ketamine-induced amnesia by blockade of GABA-A receptor in the medial prefrontal cortex of mice. *Neuroscience* **2017**, *344*, 48–55. https://doi.org/10.1016/j.neuroscience.2016.02.056
67. Davidson, A.; deGraaff, J.C. Anesthesia and Apoptosis in the Developing Brain: An Update. *Curr. Anesthesiol. Rep.* **2013**, *3*, 57–63. https://doi.org/10.1007/s40140-012-0006-1
68. Lisek, M.; Mackiewicz, J.; Sobolczyk, M.; Ferenc, B.; Guo, F.; Zylinska, L.; Boczek, T. Early Developmental PMCA2b Expression Protects From Ketamine-Induced Apoptosis and GABA Impairments in Differentiating Hippocampal Progenitor Cells. *Front. Cell Neurosci.* **2022**, *16*, 890827. https://doi.org/10.3389/fncel.2022.890827
69. Shahidi, S.; Hashemi-Firouzi, N.; Afshar, S.; Asl, S.S.; Komaki, A. Protective Effects of 5-HT1A Receptor Inhibition and 5-HT2A Receptor Stimulation Against Streptozotocin-Induced Apoptosis in the Hippocampus. *Malays. J. Med. Sci.* **2019**, *26*, 40–51. https://doi.org/10.21315/mjms2019.26.2.5
70. Pham, T.H.; Gardier, A.M. Fast-acting antidepressant activity of ketamine: highlights on brain serotonin, glutamate, and GABA neurotransmission in preclinical studies. *Pharmacol. Ther.* **2019**, *199*, 58–90. https://doi.org/10.1016/j.pharmthera.2019.02.017
71. Frans, Ö.; Rimmö, P.A.; Åberg, L.; Fredrikson, M. Trauma exposure and post-traumatic stress disorder in the general population. *Acta Psychiatr. Scand.* **2005**, *111*, 291–299. https://doi.org/10.1111/j.1600-0447.2004.00463.x
72. CB-Dock2. Cavity Detection Guided Blind Docking. Available online: https://cadd.labshare.cn/cb-dock2/index.php (accessed on 07 January 2025).
73. RCSB PDB - 5ZTY: Crystal structure of human G protein coupled receptor. Available online: https://www.rcsb.org/structure/5ZTY (accessed on 9 January 2025).
74. RCSB PDB - 6HUP: CryoEM structure of human full-length α1/β3/γ2L GABA(A)R in complex with diazepam (Valium), GABA and megabody Mb38. Available online: https://www.rcsb.org/structure/6hup (accessed on 7 November 2025).
75. RCSB PDB - 5ZKB: Crystal structure of rationally thermostabilized M2 muscarinic acetylcholine receptor bound with AF-DX 384. Available online: https://www.rcsb.org/structure/5ZKB (accessed on 8 January 2025).
76. RCSB PDB - 6CM4: Structure of the D2 Dopamine Receptor Bound to the Atypical Antipsychotic Drug Risperidone. Available online: https://www.rcsb.org/structure/6CM4 (accessed on 9 January 2025).
77. RCSB PDB - 8FYX: Buspirone-bound serotonin 1A (5-HT1A) receptor-Gi1 protein complex. Available online: https://www.rcsb.org/structure/8FYX (accessed on 8 January 2025).
78. RCSB PDB - 7XTC: Serotonin 7 (5-HT7) receptor-Gs-Nb35 complex. Available online: https://www.rcsb.org/structure/7XTC (accessed on 8 January 2025).
79. RCSB PDB - 3LSX: Piracetam bound to the ligand binding domain of GluA3. Available online: https://www.rcsb.org/structure/3LSX (accessed on 13 January 2025).
80. RCSB PDB - 4K5Y: Crystal structure of human corticotropin-releasing factor receptor 1 (CRF1R) in complex with the antagonist CP-376395. Available online: https://www.rcsb.org/structure/4K5Y (accessed on 9 January 2025).

 doi:10.20944/preprints202504.0388.v1

81. RCSB PDB - 4OO9: Structure of the human class C GPCR metabotropic glutamate receptor 5 transmembrane domain in complex with the negative allosteric modulator mavoglurant. Available online: https://www.rcsb.org/structure/4OO9 (accessed on 9 January 2025).
82. Shabelnyk, K.; Fominichenko, A.; Antypenko, O.; Gaponov, O.; Kamyshnyi, O.; Belenichev, I.; Yeromina, H.; Antypenko, L.; Kovalenko, S. Antistaphylococcal triazole-based molecular hybrids: design, synthesis and activity. *Pharmaceuticals* **2025**, *18*, 83. https://doi.org/10.3390/ph18010083
83. ProTox-II - Prediction Of Toxicity Of Chemicals. Available online: https://tox-new.charite.de/protox_II/index.php?site=home.-do (accessed on 11 May 2024).
84. SwissADME. Available online: http://www.swissadme.ch/ (accessed on 16 May 2024).
85. Belenichev, I.; Bukhtiyarova, N.; Ryzhenko, V.; Makyeyeva, L.; Morozova, O.; Oksenych, V.; Ryzhenko, O.; Suprun, E.; Kamyshnyi, O. Methodological Approaches to Experimental Evaluation of Neuroprotective Action of Potential Drugs. *Int. J. Mol. Sci.* **2024**, *25*, 10475. https://doi.org/10.3390/ijms251910475